ACS APPLIED MATERIALS & INTERFACES

www.acsami.org

Review

Processable Conjugated Microporous Polymer Gels and Monoliths: Fundamentals and Versatile Applications

Songhao Luo, Eydhah Almatrafi, Lin Tang, Biao Song, Chengyun Zhou, Yuxi Zeng, Guangming Zeng,* and Zhifeng Liu*

Cite This: *ACS Appl. Mater. Interfaces* 2022, 14, 39701−39726

Read Online

ACCESS | Metrics & More | Article Recommendations

ABSTRACT: Conjugated microporous polymers (CMPs) as a new type of conjugated polymers have attracted extensive attention in academia and industry because of the combination of microporous structure and π-electron conjugated structure. The construction and application of gels and monoliths based on CMPs constitute a fertile area of research, promising to provide solutions to complex environmental and energy issues. This review summarizes and objectively analyzes the latest advances in the construction and application of processable CMP gels and monoliths, linking the basic and enhanced properties to widespread applications. In this review, we open with a summary of the construction methods used to build CMP gels and monoliths and assess the feasibility of different preparation techniques and the advantages of the products. The CMP gels and monoliths with enhanced properties involving various special applications are then deliberated by highlighting relevant scientific literature and discussions. Finally, we present the issues and future of openness in the field, as well as come up with the major challenges hindering further development, to guide researchers in this field.

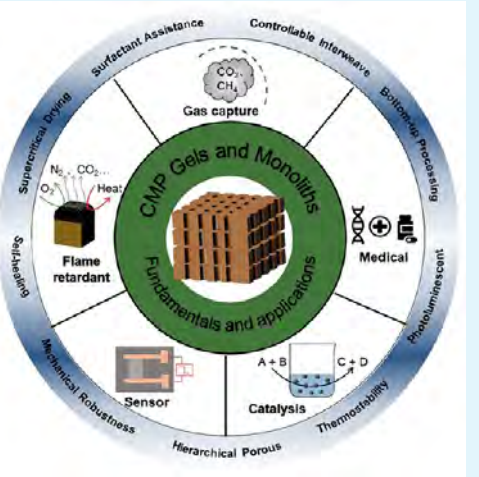

KEYWORDS: *conjugated microporous polymers, gels, supercritical drying, processability, hierarchical porous, advanced applications*

1. INTRODUCTION

Conjugated microporous polymers (CMPs) are emerging conjugated polymers with inherent microporous structure and unique π-electron conjugated structure,[1−5] which are considered strong candidates for solving global environmental and energy issues. Compared to the already grown crystalline metal−organic frameworks (MOFs)[6−8] and covalent organic frameworks (COFs)[9−12] as well as the existing porous materials,[13−16] the unique advantages of the CMP family are mainly that the amorphous properties allow the use of more abundant building units and more flexible synthetic means to explore the interaction of the extended π-conjugate framework with the micropores.[17−19] The flexibility of the design leads to mutative chemical and structural properties, thus affecting potential applications[20−24] including gas adsorption, heterogeneous catalysis, light harvesting, and energy storage.

Given the complex external environment and diversified application requirements, processable gels and monoliths are expected to flourish.[15,25,26] To improve the processability and applicability, researchers have explored various forms of CMPs such as soluble CMPs[27−29] and CMP thin films.[30−32] The main advantage of the CMP platform is the flexible design to control the microstructure and macrostructure of the CMP-based materials at the molecular level. Therefore, introducing the rigid supercrosslinking properties of CMPs into traditional gelatinous and monolithic skeletons is feasible, thus expanding the family of CMP materials.

The key points in the development of CMP gels and monoliths are to address the vulnerability and unprocessability of the original powdery CMP.[29,33−36] With careful design, the processable CMP gels and monoliths are expected to show amazing potential in widespread applications.[37−40] The timeline of major milestones toward advancement in CMP gels and monoliths is illustrated in Figure 1.

Reviewing the CMP materials family, the processability and device integration has been identified as the great challenges in this field. To explore the wider application range of the CMP materials family and achieve interesting combinations of porosity and conjugation, researchers in the interdisciplinary field have made a joint effort for these challenges. In 2011, Li

Received: June 7, 2022
Accepted: August 15, 2022
Published: August 25, 2022

https://doi.org/10.1021/acsami.2c10088
ACS Appl. Mater. Interfaces 2022, 14, 39701−39726

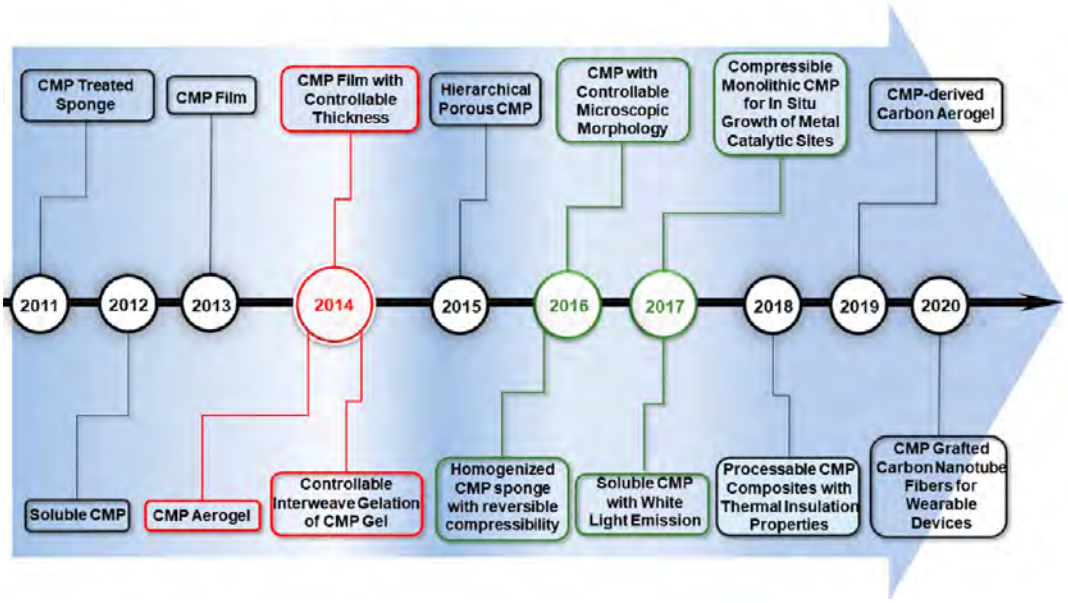

Figure 1. Selected quintessential processable CMPs at different time periods: 2011;[33] 2012;[27] 2013;[30] 2014;[29,31,34,41] 2016;[42,43] 2017;[44,45] 2018;[38] 2019;[39] 2020.[46]

et al.[33] used a sponge with a macropore structure to provide support for the synthesis of CMPs and obtained the processable CMP treated sponge for the first time, which is a good start in this field. Andrew I. Cooper, one of the pioneers of the CMP family, led the synthesis of the first soluble CMP, which can be further processed from solution into thin films.[27] Gu et al. provided a new electrochemical approach to preparing CMP films, achieving precise control of the electrochemical properties of carbazole-based CMP films,[30] and further achieving comprehensive control of the thickness of these films.[31] These films have high cross-linking degrees, remarkable electrochemical properties, and rapid responsiveness, showing great potential in organic photovoltaic cells and high-sensitivity sensor applications.[30,31]

In 2014, the concept of CMP aerogel was first proposed by Du et al.,[34] and the CMP composite gel interlaced with two components was first formed by Wang et al. in a knitting manner,[29] whose pore characteristics can be adjusted by changing monomer concentration, reaction temperature, and solvent type. Subsequently, Tan et al.[41] synthesized a layered porous structure with micropores, mesopores, and macropores by knitting, and Bao et al. further demonstrated that adjusting the mole ratio of the synthetic monomer for CMPs could not only adjust the pore characteristics of the CMPs but also adjust their thermal stability and microstructure.[42] In 2016, Kim et al. synthesized CMP-based sponges using a homogenized electrospun nanofiber as the reinforcement for rapid adsorption of organic dyes in water[43] and further synthesized fluoride-functionalized CMP-based sponges supported Ag metal nanocatalysts for rapid removal of 4-nitrophenol from water[44] in the following year.

Also in 2017, Patra et al.[45] synthesized soluble, processable, multifunctional CMPs based on tetraphenylcyclopentadiene. The polymers not only have gas adsorption properties but also have strong tunable luminescence properties,[45] which extends the application of the CMP family in the optical field. In 2018, Li's group reported for the first time novel CMPs containing benzotriazole moiety monomers, which have excellent thermal insulation performance and is considered a promising thermal insulation material.[38] In 2019, they also found that a class of biphenyl CMP-derived carbon aerogels, which not only retain low thermal conductivity (0.192 W m^{-1} K^{-1}) but also have excellent photothermal conversion performance (86.8% under 1 Sun irradiation) and are considered as candidate materials for a variety of photothermal conversion applications such as distillation, desalination, and the production of fresh water.[39] In 2020, Liao et al.[46] successfully grafted a polytriphenylamine-based CMP network to carbon nanotube fibers to prepare all-solid-state wheel-twisted fiber-shaped supercapacitors. The supercapacitor has high area specific capacitance (671.9 mF cm^{-2} at a current density of 1 mA cm^{-2}) and excellent stability (retaining 84.5% of the initial capacitance after 10 000 bending cycles),[46] which opens up a way for the application of the CMP family in wearable electronic devices.

Cooper reviewed the research progress of CMPs in 2009 and emphasized the potential applications of these materials in the future.[3] CMPs allow functional exploration of π-conjugated frameworks and nanopores to meet challenges in gas adsorption, heterogeneous catalysis, luminescence, light harvesting, and electric energy storage. In 2012, Vilela et al.[47] presented the challenges faced by the synthesis, characterization, and testing of CMPs in areas such as energy conversion and production, with special emphasis on the morphological control aspects of CMPs and the significance of these properties in energy applications. In 2013, Jiang et al.[5] further reviewed the progress in molecular design principle, synthesis, and structural research, and came up with the frontier of potential applications of CMPs, to promote the rapid development of the materials.

Recently, Lee and Cooper reviewed the progress in gas adsorption, chemical encapsulation, photocatalysis, photoemission, sensing, energy storage, biological application, and solar fuel production since the beginning of CMP research, and proposed the future development prospects of these materials.[48] They also compared the prospects of CMPs with the growing of conjugated crystalline COFs. Vilela et al.[49] highlight the selection work of CMPs, including basic structural design principles, various synthetic schemes, and

https://doi.org/10.1021/acsami.2c10088
ACS Appl. Mater. Interfaces 2022, 14, 39701−39726

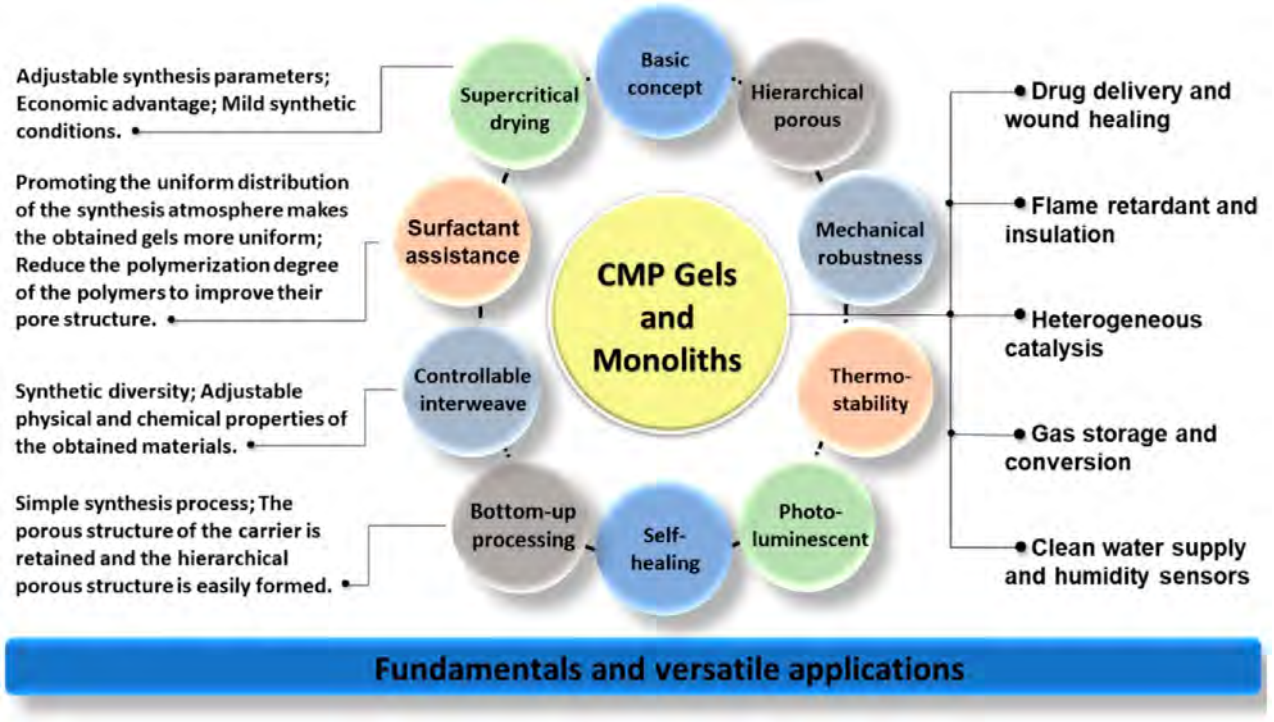

Figure 2. Diagram summary of the fundamentals and versatile applications of conjugated microporous polymer gels and monoliths.

Table 1. Main Construction Methods for the Formation of CMP Gels and Monoliths

methods	methodology elaboration	representative samples	S_{BET} ($m^2\ g^{-1}$)	V_{total} ($cm^3\ g^{-1}$)	ref
supercritical drying	advantages: adjustable synthesis parameters, economic advantage, mild synthetic conditions; deficiencies: low mechanical strength of the obtained materials	PTEB	1701	1.01	34
		TPM-BD-CMP	1008	0.50	54
		RGO-*g*-P_3HT	523	~34[a]	55
		PDVB-BF_4IL	417	0.50	56
surfactant assistance	advantages: promoting the uniform distribution of the synthesis atmosphere makes the obtained gels more uniform, reducing the polymerization degree of the polymers to improve their pore structure; deficiencies: increased synthetic conditions; surfactant consumption	PTEB-F-5[b]	1027	0.96	51
		SMCP			57
		An-CPOP-2[c]	1130	1.02	58
		CMP-TST	432.3		59
controllable interweave	advantages: synthetic diversity; adjustable physical and chemical properties of the obtained materials; deficiencies: unmanageable reaction conditions	ZnTEPP	906.4	0.43	29
		MP-0.8	463	0.17	60
		MPN	1800	1.60	61
		PTEPE-TBPE	1083	1.51	62
		CMP-BT	217.9	0.71	63
		CMP-F	316.8		64
bottom-up processing	advantage: simple synthesis process; porous structure of the carrier is retained and the hierarchical porous structure is easily formed; deficiencies: poor application stability of the obtained material	HCMP-1	955		33
		HCMP-2	928		33
		PVASi@TEDB-NH_2	447		43
		CMP-H	340	0.23	52
		PUS-MOP-A	306		53

[a]Approximately 34 $cm^3\ g^{-1}$ vs 0.15−2.81 $cm^3\ g^{-1}$ from micro- and mesoporous conjugated polymers. [b]With an initial fluorosurfactant concentration of 5 mg mL^{-1}. [c]9,10-Bis(diphenylmethylene)-9,10-dihydroanthracene as the building unit with 2,4,6-trichloro-1,3,5-triazine as external cross-linkers; PTEB, poly(1,3,5-triethynylbenzene); TPM, tetrakis(4-ethynylphenyl)methane; BD, butadiynylene; RGO, reduced graphene oxide; P3HT, poly(3-hexylthiophene); PDVB, polydivinylbenzene; IL, ionic liquid; SMCP, sulfonated microporous conjugated polymer; TST, tristyryl-s-triazine unit; ZnTEPP, polymeric 5,10,15,20-tetra(4-ethynylphenyl)porphyrin-Zn(II)); MP-0.8, which was synthesized using a 0.8:1 molar ratio of bis(bromothiophene) monomer to 1,3,5-triethynylbenzene; MPN, microporous polymer network; TEPE, 1,1,2,2-tetrakis(4-ethynylphenyl)ethene; TBPE, 1,1,2,2-tetrakis(4-bromophenyl)ethene; CMP-BT, benzothiadiazole-based conjugated microporous polymer; CMP-F, fluorine-containing conjugated microporous polymers; PVASi@TEDB-NH_2, the compressible MOP composite produced by 2,5dibromoaniline and 1,3,5-triethynylbenzene in a dispersion of homogenized PVASi nanofibers; CMP-H, nanotube-like CMP by one-step chemical synthesis via cross-coupling of 1,4-diethynylbenzene and 2,4,6-tribromophenol; PUS-MOP-A, which was prepared by carrying out Sonogashira−Hagihara coupling reaction of 1,3,5-triethynyl benzene, 1.4-diiodobenzene, and 2,5-diiodobenzoic acid in a polyurethane sponge.

https://doi.org/10.1021/acsami.2c10088
ACS Appl. Mater. Interfaces 2022, 14, 39701−39726

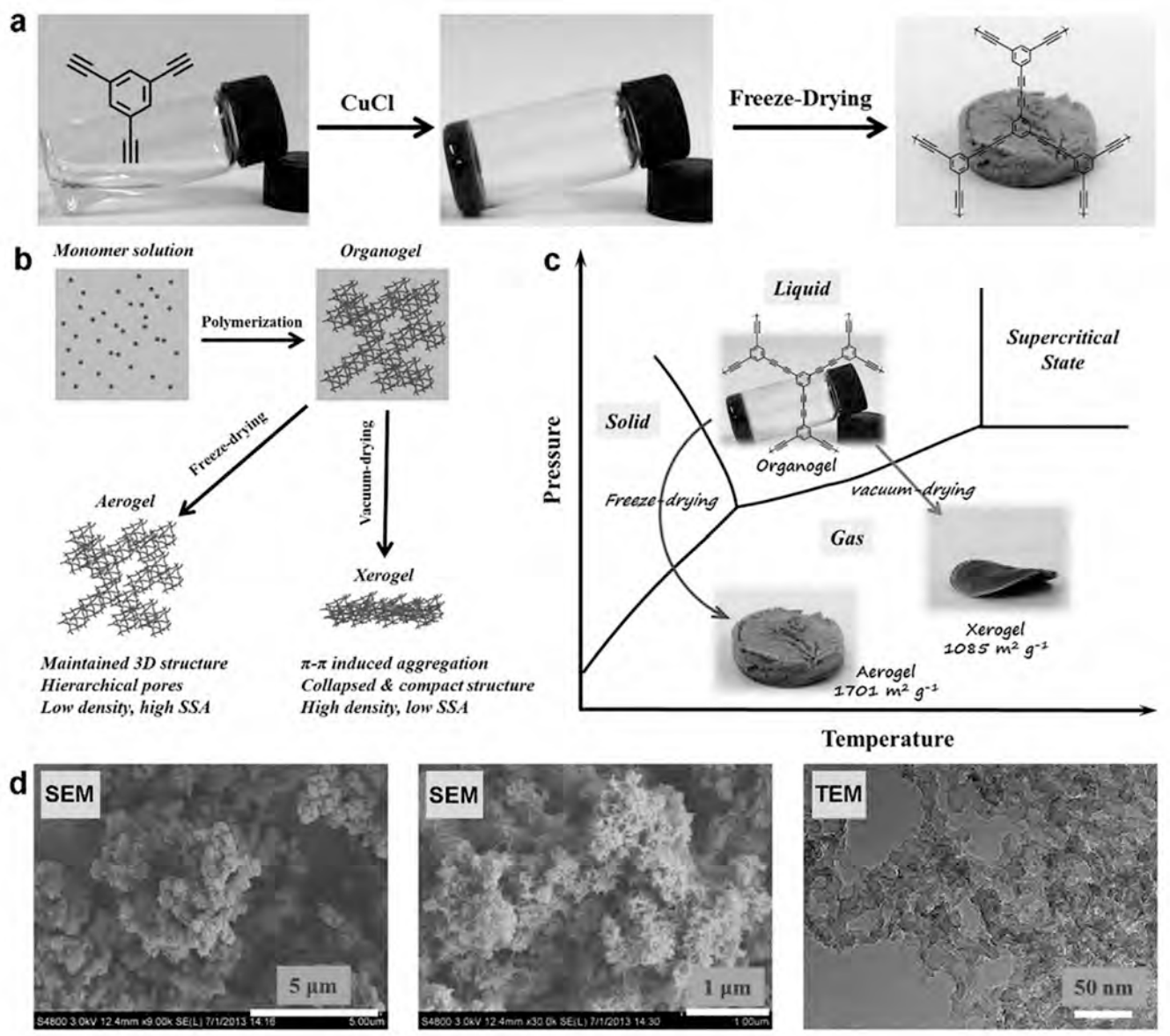

Figure 3. Supercritical drying technology for conjugated microporous polymer aerogels. (a) Schematic demonstration of the synthetic route toward the PTEB aerogel via Glaser coupling reactions and a following freeze-drying process. (b) Schematic illustration of the structure and preparation procedures of supercritical drying, and (c) demonstration of monolithic and porous PTEB aerogels acquired from corresponding organogels via freeze-drying, which differs from traditional vacuum drying in avoiding directly crossing the gas−liquid phase line. (d) SEM images and TEM images of the aerogel obtained from freeze-drying. Reproduced with permission from ref 34. Copyright 2014 Wiley−VCH.

up-to-date applications of these common CMP materials. To accelerate the development of CMPs in the field of clean energy, we comprehensively reviewed the latest progress of CMPs in the field of clean energy,[18] including hydrogen storage, carbon dioxide capture, metal-ion rechargeable batteries, supercapacitors, fuel cells, and photovoltaic cells, presenting the assembly principles and methods of CMP-nanoparticles (NPs), nanotubes (NTs), and thin films, also introduced the computer simulation methods for predicting and guiding the synthesis and application of CMPs.

With the development of science and technology, processable gels and monoliths are expected to flourish.[15] CMPs as a design platform, the rigid supercrosslinking properties can be introduced into the traditional gel and monolith frameworks, and the microstructure and macroscopic structure of the networks can be fundamentally controlled by adjusting the reaction conditions and the ratio of reaction monomers.[50] The field of research is still in its infancy, so this review aims to provide a comprehensive and solid introduction to the development of CMP gels and monoliths, including the latest breakthroughs and their impact on the wider scientific community, which will give individuals a quick understanding of this field and make joint efforts to promote the development of this field. In this review, we summarize the up-to-date progress in the construction of CMP gelatinous and monolithic structures, illuminating the feasible formation mechanisms as well as the unique properties of CMP gels and monoliths (Figure 2). We then describe the widespread applications of CMP gels and monoliths including biomedical, flame-retardant insulation materials, heterogeneous catalysis, carbon dioxide fixation, water purification, and sensors. Finally, we address the open issues in this field and present future perspectives. We

https://doi.org/10.1021/acsami.2c10088
ACS Appl. Mater. Interfaces 2022, 14, 39701−39726

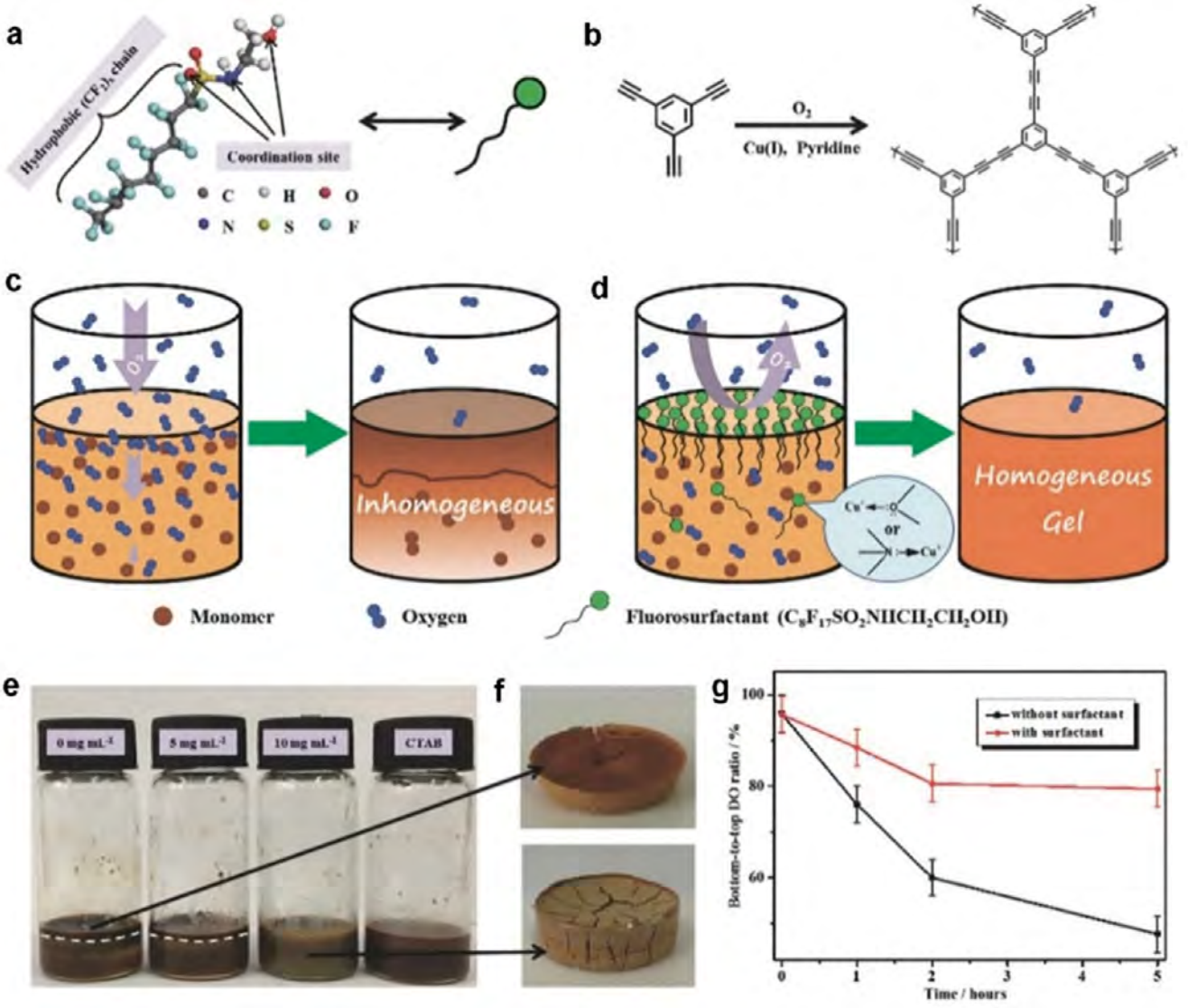

Figure 4. Illustration of synthetic strategy for homogeneous CMP aerogels by a fluorosurfactant-assisted Glaser coupling reaction. (a) Molecular structure and the functions of the employed fluorosurfactant. (b) Reaction conditions of the Glaser coupling reaction (Hay's condition). (c, d) Schematic diagrams of the gelation mechanism for PTEB gels without and with fluorosurfactants, respectively. (e) PTEB wet gel with different initial fluorosurfactant concentrations (three samples on the left) and with 10 mg mL^{-1} CTAB. The white dashed line indicates the interface between the top dark gel layer and the bottom light gel. (f) Corresponding aerogels after freeze-drying. (g) In situ ratio of bottom-to-top dissolved oxygen (DO) variation with time evolution. Reproduced with permission from ref 51. Copyright 2015 Wiley–VCH.

hope that this review will inspire researchers in the materials fields to come up with innovative ideas for new materials and applications based on processable CMP gels and monoliths.

2. CONSTRUCTION PRINCIPLES AND METHODS

Processable CMP gels and monoliths provide a platform to independently control the macroscopic shape and chemical composition of CMP materials, which has the potential to extend the properties and applications of CMPs. This section introduces the required knowledge in the construction of CMP gels and monoliths, including freeze-drying synthesis of CMP aerogels,[34] assisted synthesis of CMP wet gels,[51] the manufacture of the CMP-treated foams and sponges, etc.[33,52,53] The main construction methods are summarized in Table 1. Conceptually, these methods can be extended to existing CMPs to form processable CMP gels or monoliths. There is still a lot of clarification to be made around the basic requirements for CMP gel and monolith formation. Generally, the CMP monoliths are composed of processable matrix monoliths and CMP fillers. The CMP gels are three-dimensional (3D) bulk materials consisting only of cross-linked nanoscale CMPs, which are a branch of amorphous CMPs.

2.1. Supercritical Drying. Supercritical drying technology can improve the pore structure of polymer gels and monoliths.[65] Among them, the freeze-drying process dries the samples by solvent sublimation.[66] The polymer was synthesized by Glaser coupling reactions and then used the freeze-drying process to form an aerogel with abundant porosity (Figure 3a). Compared to homogeneous coupling reactions that require inert gas protection,[67−70] this strategy can be carried out under mild conditions and atmospheric connectivity. On this basis, this method has certain economic advantages. Noteworthily, the atmospheric air plays a critical role in the formation of CMP gel. Therefore, the external atmospheric environment needs to be kept stable during the reaction process to facilitate the uniform formation of the CMP gel.

Theoretically, the freeze-drying procedure does not damage the properties of the material itself.[34,66] In the drying procedure, because the solvent sublimation process bypasses the gas–liquidus (Figure 3b,

https://doi.org/10.1021/acsami.2c10088
ACS Appl. Mater. Interfaces 2022, 14, 39701−39726

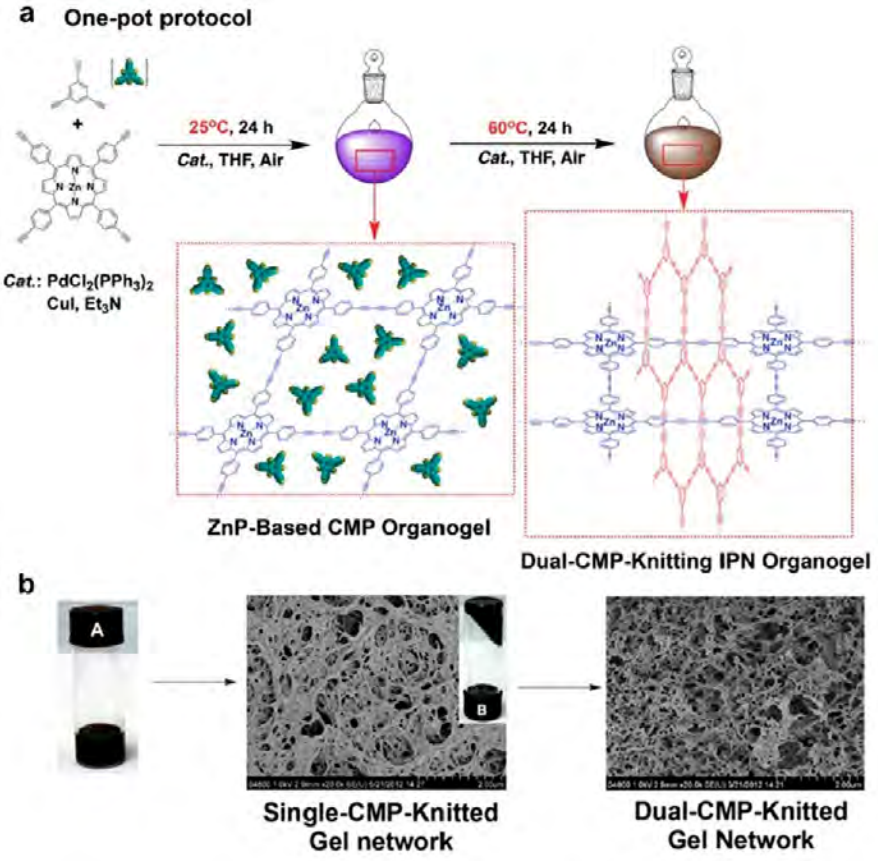

Figure 5. Adjust the monomer concentration, reaction temperature, and solvent type to prepare the CMP xerogels with adjustable microporosity. (a) Controllable interweave processing for the CMP xerogels (b). Corresponding SEM images of fibrous ZnP framework xerogel and CMP-interwoven interpenetrating xerogels. The insets show (A) the THF solution of reaction mixtures and (B) the ZnP organogel after the alkyne homocoupling reaction, respectively. Reproduced with permission from ref 29. Copyright 2014 American Chemical Society.

c),[34] the dramatic change in polymer surface tension is avoided. Thus, the size shrinkage and internal structure collapse caused by the aggregation of polymers is effectively inhibited. Finally, polymer gels and monoliths with hierarchical porous structures are obtained (Figure 3d, including micro/nanopores and interconnected macropores). This strategy could provide an unparalleled opening for the development of CMPs to improve the properties from powdery to a processable phase.

2.2. Surfactant Assistance. For surfactant assistance, the introduction of surfactant mainly has the following functions:[46,51,53] The surfactant adsorbs at the gas−liquid interface and can prevent oxygen from entering the solution from the air during the polymerization process, ensuring uniform dissolved oxygen in the solution and making the synthetic polymer gel more uniform. The surfactant can coordinate with the catalysts to reduce the degree of polymerization and eventually change the pore structure; the functional group chains of the surfactant can also increase the hydrophobicity of the resulting polymer gel. For instance, the fluorosurfactant is introduced into the Glaser coupled reaction system to synthesize the CMP wet gel in an O_2 atmosphere (Figure 4a, b).[51] The existence of fluorosurfactant is beneficial to the uniform distribution of dissolved oxygen (Figure 4g), and the latter is vital to obtaining a uniform gel.

The interfacial reaction at the gas−water interface rapidly forms a dense gel layer due to the abundant dissolved oxygen, which may hinder the subsequent oxygen penetration and uniform distribution, leading to an inhomogeneous gel or even no formation (Figure 4c). In contrast, when fluorosurfactants are present, the gas−water interface is isolated by the surfactant/catalyst ligands to prevent the reaction system with uniform dissolved oxygen distribution from being disturbed by air, thus forming a homogeneous gel (Figure 4d). Meanwhile, the content of the surfactant influences gels formation. To illustrate, a sufficient fluorosurfactant is more conducive to capturing catalyst to obtain a more uniform gel by reducing the degree of polymerization (Figure 4e, f).

2.3. Controllable Interweave Methods. Controllable interweave methods to construct processable pure CMP gels include adjusting the monomer type and the molar ratio as well as reaction conditions such as the reaction temperature and the solvent. In 2016, Li's research group controlled the formation of a CMP aerogel by adjusting the ratio of alkynyl and bromine functional groups in the monomers.[42] When the ratio is 1.5:1, the microstructure of the polymer is mainly composed of many nanospheres and a small number of nanotubes. When the ratio is 3:1, the opposite situation occurs. When the ratio is increased to 5:1, the CMP is composed of pure nanotube structures and forms a tight gel structure. Finally, when the monomer ratio is further increased to 9:1, the CMP is composed of amorphous nanoparticles.

Appropriate reaction conditions can promote the monomer and catalyst to form a homogeneous solution phase, while the adjustment of the monomer can accelerate the transition of the solution phase to the gel phase, both of which lead to controllable interweaving to form a porous gel morphology.[29,71,72] As shown in Figure 5a, the sequential interpenetrating CMP xerogel network was synthesized by changing the poly(aryleneethynylene) (PAE) and Zn^{II}-porphyrin-based (ZnP) network content as well as the reaction temperature and the solvent type. Increasing the temperature can accelerate the gelation of the PAE network, during which temperature-controlled sequential polymerization is used to further form the CMP woven interpenetrating network organogels. First, the ZnTEPP monomer and TEB were polymerized at 25 °C for 24 h under the action of a catalyst to form a ZnP-based CMP network. The reaction was then heated to

https://doi.org/10.1021/acsami.2c10088
ACS Appl. Mater. Interfaces 2022, 14, 39701−39726

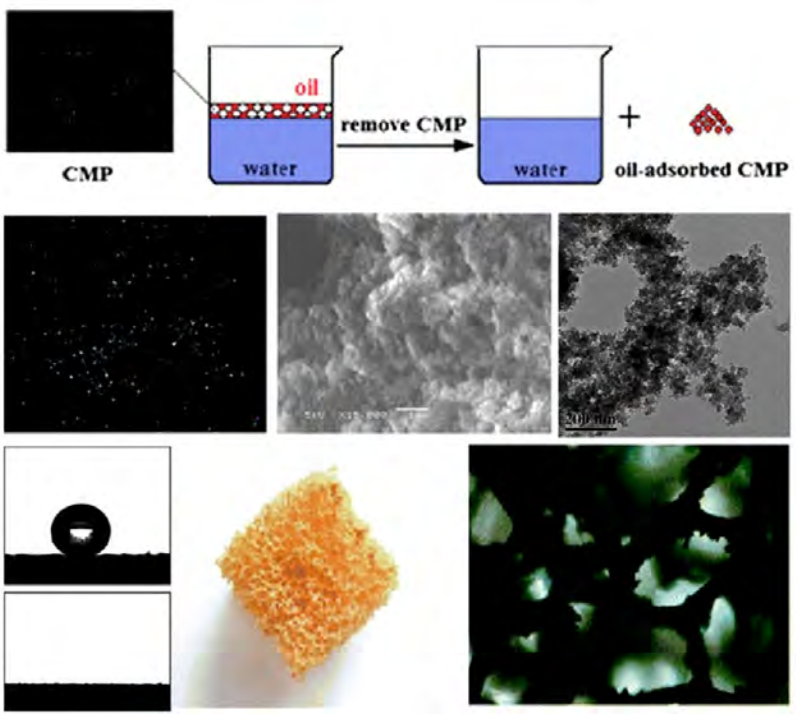

Figure 6. Superhydrophobic conjugated microporous polymer treated sponge. From left to right are simulation structure, SEM image, and TEM image of the HCMP-1 (top), as well as the measurement of contact angle with water and with diesel oil for the HCMP-1, camera image of the HCMP-1 treated sponge, and optical microscopy image of the HCMP-1 treated sponge (below). Reproduced with permission from ref 33. Copyright 2011 Royal Society of Chemistry.

60 °C, and the immobilized TEB monomer was polymerized in ZnP-based CMP organogels to form double CMP interpenetrating networks, thus forming completely rigid dual-CMP-knitting xerogels.

Many common organic solvents are suitable for the internal interweaving of CMP gels, such as tetrahydrofuran, dimethylformamide, acetone, dioxane, toluene, and dimethyl sulfoxide.[29] The CMP xerogels present an interwoven fibrous network of microstructures (Figure 5b) after removing the organic solvent. Meanwhile, the pore properties of CMP xerogels can be effectively adjusted by adjusting the ratio of PAE and ZnP (Figure 5b). This provides a feasible strategy for bridging the difference in the specific surface area and the pore size distribution between the amorphous porous polymer and crystalline ordered porous material such as MOFs and COFs. Furthermore, bearing in mind the flexibility and controllability of the interweaving process and the inherent extended π-conjugate network, the processable CMP gels present broader future applications than powdery CMPs as well as ordinary MOFs and COFs.

Given the future applications, the CMP gels synthesized by the controllable interweave also show enhanced mechanical robustness for further processing.[36,60] For instance, the compressible CMP gel was prepared using a conventional Sonogashira−Hagihara reaction of 1,3,5-triethynylbenzene (TEB) and the bis(bromothiophene) monomer (PBT-Br) and by adjusting the ratio of the two monomers,[60] which has strong mechanical strength and remains essentially unchanged after 10 cycles of repeated stress loading and unloading. Furthermore, to meet the diversity of application needs, different shapes of ultralightweight CMP gels can be constructed,[36] such as rod, line, or cylinder, which provides a feasible strategy for processable, mechanical robustness, and flexible CMP gels with special applications.

The electrospinning is used later to construct CMP gels, which is a viable and universal technique for preparing nanofibers. The method is cost-effective and scalable and is commonly used to construct nanofiber materials consisting of interpenetrating macropores, fully connected hollow structures, and densely distributed micropore networks.[73,74] CMP materials synthesized by this method have microscopic nanofiber structures, and the overall material usually has high flexibility and a high surface area to volume ratio,[61−64] which is conducive to the preparation of wearable soft electronic devices including chemical sensors and filtration membranes.

In 2015, Yuan et al. synthesized CMP composite materials by the electrospinning method and used them to prepare light-emitting nanofiber films with high flexibility.[62] Based on the high chemical sensitivity of the CMP material itself, this nanofiber film containing CMP components has been used as a sensitive environmental monitoring sensor.[62] Furthermore, compared to porous carbon without graphene templates,[62] the carbon nanomaterials obtained from the pyrolysis of the CMP material exhibit an increased electrical capacity. In addition, Jing et al. recently prepared CMP composite nanomaterials using polyimide as a matrix by electrospinning.[64] The assembled CMP-based filtration membrane has high application potential in emulsion separation and shows high oil/water separation performance.

2.4. Bottom-up Processing. The bottom-up processing for the construction of CMP monoliths usually involves the following steps: A foam with rich pore and elastic properties is first immersed into the synthetic precursors of CMP, then make the foam or sponge in the soaking and reaction by CMP networks securely wrapped and penetration, the final cleaning and drying product. In 2011, Li's group prepared CMP sponge composites using commercial polyurethane sponges physically adsorbing the self-assembling HCMPs (homocoupling polymerization of 1,3,5-triethynylbenzene and/or 1,4-diethynylbenzene).[33] The CMP sponges have superhydrophobic/oil-wet properties due to the use of monomers with corresponding properties as well as retaining the interpenetrating pore of the original sponge (Figure 6). This opens the door to a new world of processable CMP monoliths.

Subsequently, Tan's group prepared the CMP-treated foams using a commercial polyurethane sponge as the carrier by in situ Sonogashira−Hagihara reaction of 1,4-diethynylbenzene with 2,4,6-tribromophenol.[52] As well as Chang et al. prepared a compressible CMP sponge composite (PUS-MOP-A) by in situ polymerization of carboxyl-containing 2,5-diiodobenzoic acid, 1,3,5-triethynyl benzene, and 1,4-diiodobenzene on a block and compressible polyurethane

https://doi.org/10.1021/acsami.2c10088
ACS Appl. Mater. Interfaces 2022, 14, 39701−39726

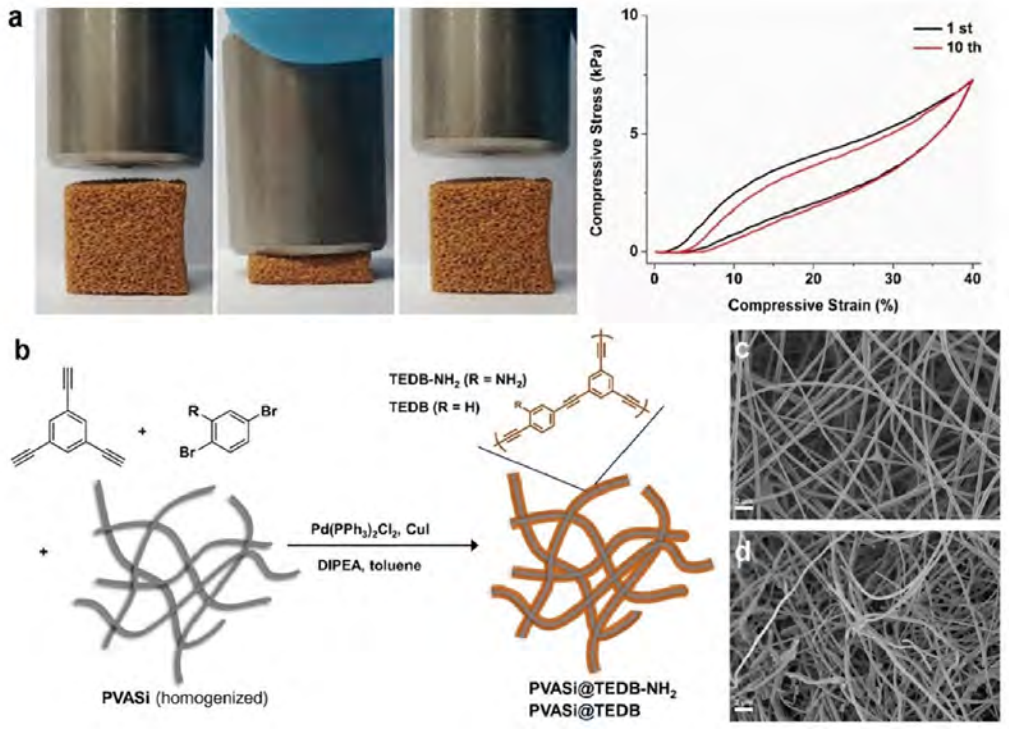

Figure 7. Compressible conjugated microporous polymer treated foam. (a) Sequential images of PUS-MOP-A in as-prepared, compressed, and released states. Reproduced with permission from ref 53. Copyright 2017 Elsevier. (b) Synthesis of PVASi@TEDB-NH_2 and PVASi@TEDB. SEM images of PVASi (c) before and (d) after homogenization. Reproduced with permission from ref 43. Copyright 2016 Elsevier.

sponge (Figure 7a).[53] The porous composites were transformed from superhydrophobic to superhydrophilic by KOH treatment,[53] which could provide more accessible catalytic active sites for photocatalysis. Furthermore, Chang et al. used the PVA-silica nanofiber (PVASi) obtained from poly(vinyl alcohol) (PVA) and tetraethyl orthosilicate (TEOS) as a substrate to prepare a compressible CMP-based foam with core−shell structure by an in situ Sonogashira−Hagihara reaction of 2,5-dibromoaniline with 1,3,5-triethynylbenzene (Figure 7b).[43] This compressible property could be attributed to the retention of the cross-linked structure (Figure 7c, d) of the original foam by the CMP-based foam.

In conclusion, the infiltration property of the carrier material should be considered in the bottom-up processing. The carrier does not affect the chemical properties and adsorption properties of CMP composite monoliths. Due to the combination of porous carrier and CMP material by purely physical interaction, this composite material has poor application stability under harsh conditions. Therefore, the researchers developed in situ polymerization and interweave strategies for the synthesis of pure CMP gels and monoliths. In the process of interweaving, attention should be paid to the effects of monomer type and proportion as well as reaction conditions on gel formation. Finally, to eliminate the influence of polymer surface tension and promote uniform gel synthesis, supercritical drying technology, and surfactant-assisted method are used.

3. BASIC AND ENHANCED PROPERTIES

3.1. Basic Concept. Compared with CMP powders, the reported CMP gels and monoliths demonstrate outstanding ductility, as well as structural and chemical properties, which facilitate their further application. CMP monoliths usually inherit the outstanding processability and elasticity of matrix materials and have a bright application prospect in the fields of adsorption and catalysis.[33,43,52,53] CMP gels are synthesized from pure CMP by adjusting the reactive monomer and reaction conditions, which are new gels with both CMPs and bulk characteristics.

Among them, CMP hydrogels have 3D conjugated networks composed of cross-linked hydrophilic polymers and biopolymers or nanofibers,[75−77] which have a wide range of applications in biomedical applications including drug delivery, tissue engineering, and wound healing. Aerogels are 3D porous solid networks that can be transformed from hydrogels,[78,79] and the conversion process usually requires a special drying process to ensure that the microstructure and macroscopic size of the aerogel remain stable before and after drying.

In 2014, the concept of "CMP aerogel" was proposed for the first time.[34] The CMP aerogels have higher porosity and remarkable adsorption performance than most CMP-based materials developed at present.[34,51] The emergence marks a step forward in the field of synthesis and engineering applications of CMP materials. Processing CMPs into arbitrary shapes and structures has the potential to bring interesting properties to them. Compared with common powdered CMPs or other gels and monoliths, processable CMP gels, and monoliths have enhanced properties such as hierarchical porous structure, mechanical robustness, and thermostability. Especially, the π-conjugation effect of conjugated groups in CMP gel is different from ordinary polymer gel. For these highly conjugated porous gel networks, the π-conjugation effect on the backbone of polymerization coupled with mass transfer in porous systems leads to many unique properties, including fast electron transport and highly efficient matter exchange, which promotes their applications in energy storage,[45,80,81] light-energy conversion,[39,82] and electrochemiluminescence.[83,84]

3.2. Hierarchical Porous Materials. Compared with conventional porous materials, CMPs usually have larger

https://doi.org/10.1021/acsami.2c10088
ACS Appl. Mater. Interfaces 2022, 14, 39701−39726

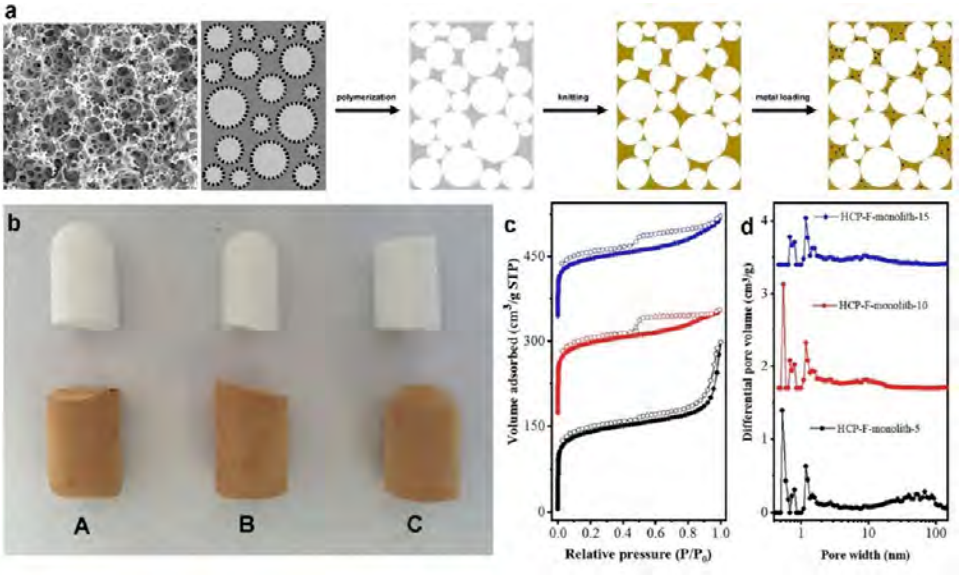

Figure 8. Functionalized hierarchical porous conjugated microporous polymer monoliths. (a) Illustration of the synthetic route for functionalized hierarchical porous polymeric monolith and metal loading. (b) Optical images of monoliths before (upper, white) and after (lower, light brown) hyper-cross-linking with different 4VP content of (A) 5, (B) 10, and (C) 15%. (c) N_2 sorption isotherms and (d) pore size distribution of HCP-F-monolith-X (X means 4VP content). Reproduced with permission from ref 88. Copyright 2020 Elsevier.

specific surface areas and more microporous structures.[33,35,85,86] Meanwhile, functionalized hierarchical porous CMP gels and monoliths can be obtained by flexible adjustment of synthesis method and/or comonomer, which have enhanced mass transferability than powdered CMP materials because the issue of diffusion inhibition caused by a single microporosity is solved.[41,87,88] As shown in Figure 8a, the macroporous precursor was prepared by copolymerization using 4-vinylpyridine (4VP), styrene (ST), and divinylbenzene (DVB) as raw materials, as well as then formed nanopores in the macroporous matrix through dimethoxymethane/formaldehyde dimethyl acetal (FDA) cross-linking reaction, thus build the hierarchical porous structure composed of connected macropores and plentiful micropores.

The interconnected macropores morphology (Figure 8a; SEM image) remains stable during the cross-linking process and after metal loading. The hierarchical porous CMP materials (Figure 8b) appear light brown and increase in size after hyper-cross-linking with 4VP. The N_2 adsorption isotherm and pore size distribution curve can reveal the pore structure in more detail (Figure 8c, d). The pore structure and specific surface area of the polymer can be easily adjusted by changing the monomer ratio. For example, the highest BET-specific surface area of the network can reach 528 $m^2\ g^{-1}$ by adjusting the dosage of 4-VP.[88] Furthermore, with the increase in the 4-VP group, the surface area decreases while the macropores still exist,[88] which may be because the increase in the pyridine group increases the hydrophilicity, resulting in the instability of the emulsion interface during the synthesis process and thus loss of the micropores. Processable CMPs with hierarchical porous catalysts or catalyst support are expected in the heterogeneous catalysis.

3.3. Mechanical Robustness. Mechanical robustness is critical to the industrial service life of the CMP monolithic nanofoams (CMP-MNs), usually in terms of the ability to remain stable under various stresses (Figure 9a).[36] Due to the permeable and cross-linked elastic open networks and the unique microstructure (Figure 9b), the mechanical robustness of the CMP monolithic nanofoams is superior to ordinary polymer gels[60,89,90] and graphene-based aerogels,[91,92] as well as comparable to aerogels based on carbon nanotube.[93,94]

The uniaxial and biaxial compression (Figure 9c, d) can demonstrate that the prepared CMP monolithic nanofoams have robust mechanical compression cycle properties. Due to the partial structural destruction and energy dissipation of the CMP monolithic nanofoam,[36] a clear hysteresis can be observed in the first compression cycle. However, no palpable hysteresis can be observed in the subsequent continuous compression cycle tests, indicating that the structure of the CMP monolithic nanofoam is stable after the first compression cycle. The mechanical robustness provides exhilarating processability and scalability for the porous polymer to promote further industrial application.

3.4. Thermostability. The CMPs are usually formed by cross-coupling, so the synthesized products have enhanced thermostability, despite the mild synthesis temperature.[4,33] The porous rigid structure of the CMPs restricts the convection of hot air, thus forming a barrier that prevents the transfer of oxygen and heat to keep the structure stable at high temperatures. For instance, the benzotriazole-based CMP (ZCMP-1) was prepared by cross-coupling polymerization with an ethynyl to bromo functional group ratio of 1:1 using toluene as solvent at 70 °C (Figure 10a), showing enhanced thermal stability at about 400 °C with a lowest peak heat release rate (pHRR) of 9.9 W g^{-1} and a lowest thermal conductivity of 0.03 W m^{-1} k^{-1}.[38]

Meanwhile, thermogravimetry analysis (TGA) (Figure 10b) showed that the increase in nitrogen-containing groups in the ZCMP networks could further increase thermal stability. Interestingly, processable gels based on the prepared ZCMPs are more conducive to shaping and application (Figure 10c). In addition, the ZCMPs reveal a rough surface in the microscopic state (Figure 10d), which can form an expansion layer at high temperatures to effectively protect the internal main material.[38] Based on the advantages, the CMPs could have a promising future in the field of green building materials.

https://doi.org/10.1021/acsami.2c10088
ACS Appl. Mater. Interfaces 2022, 14, 39701−39726

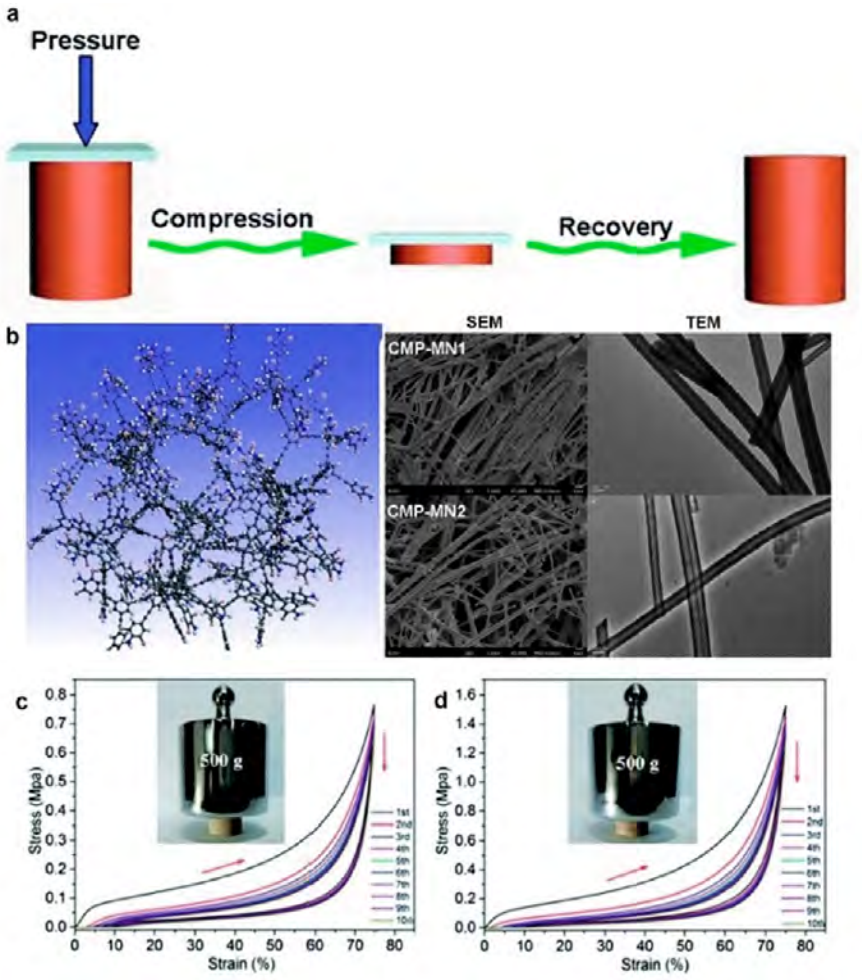

Figure 9. Monolithic nanofoams based on conjugated microporous polymer nanotubes with ultrahigh mechanical robustness. (a) Compression diagram of CMP-MNs. (b) Molecular network, SEM images, and TEM images of the CMP-MNs. (c) Compressive stress−strain curves of CMPs-MN1 for the first to the tenth test cycle. (d) Compressive stress−strain curves of CMPs-MN2 for the first to the tenth test cycle. The inset shows camera photos of CMPs-MN1 and CMPs-MN2 under 500 g weight, respectively. Reproduced with permission from ref 36. Copyright 2018 Royal Society of Chemistry, .

3.5. Photoluminescence. Photoluminescence is of great significance for the applications of materials in the fields of optics, biomedicine, and environmental monitoring. Compared with insoluble powdered CMPs,[95−97] the processable CMP-based materials have enhanced quantum yield and photoluminescence properties.[45,98] For instance, the processable photoluminescent CMP (TBDC-BZ) synthesized by tetrakis-(4-bromophenyl)-5,5-dioctyl cyclopentadiene (TBDC) with benzothiadiazole (BZ) (Figure 11a), which shows strong yellow fluorescence with a highly polar excited state in tetrahydrofuran.[45] Suitable dyes, such as 5-octyl-1,2,3,4,5-pentaphenyl-1,2-cyclopentadiene (OPCP) and perylene red (PR), are subsequently encapsulated into the TBDC-BZ matrix to form solutions, nanoparticles, gels, and films.

The spectral characteristics (Figure 11b) and the Commission Internationale de l'Eclairage (CIE) coordinates (Figure 11c) further indicate the high-quality white light emission for the processable CMP-based materials. Meanwhile, the time-resolved emission (TRES) spectra (Figure 11d) indicate the change of excitation state with delay time, which elaborate the energy transfer phenomenon between OPCP and TBDC-BZ matrix and between OPCP and PR. Interestingly, the processable CMP can be stripped to prepare transparent films, which show intense light-induced white light emission (Figure 11e), and have promising applications in optics and biomedical and environmental monitoring.

3.6. Self-Healing. Not all polymer gel systems possess self-healing properties because in many cases the valence bond interactions on the backbone of the polymerization are irreversible.[99,100] When the gel is physically damaged, the damaged surface is unable to recombine at the molecular scale under environmental conditions. In this regard, Belali et al. designed and synthesized the CMP-based chitosan hydrogel (CS/NH_2-TPP) by Schiff-base reaction using tetrakis(4-aminophenyl)porphyrin (NH_2-TPP) and 2,4,6-tris(p-formyl phenoxy)-1,3,5-triazine (TRIPOD) as monomers and chitosan as a cross-linking agent (Figure 12a).[101] Due to the dynamic imine bonds at the molecular level, the CS/NH_2-TPP hydrogel can self-healing without additional stimulation in the environment. It is noteworthy that the storage/loss modulus ratio of the CS/NH_2-TPP hydrogel decreases significantly at acidic pH (Figure 12b), which is due to the instability of imine bonds under acidic conditions.

The CS/NH_2-TPP hydrogel has a cross-linked microporous structure with a diameter of 20−30 μm and a pore wall thickness of 200−400 nm, which is stable at a stress of about

https://doi.org/10.1021/acsami.2c10088
ACS Appl. Mater. Interfaces 2022, 14, 39701−39726

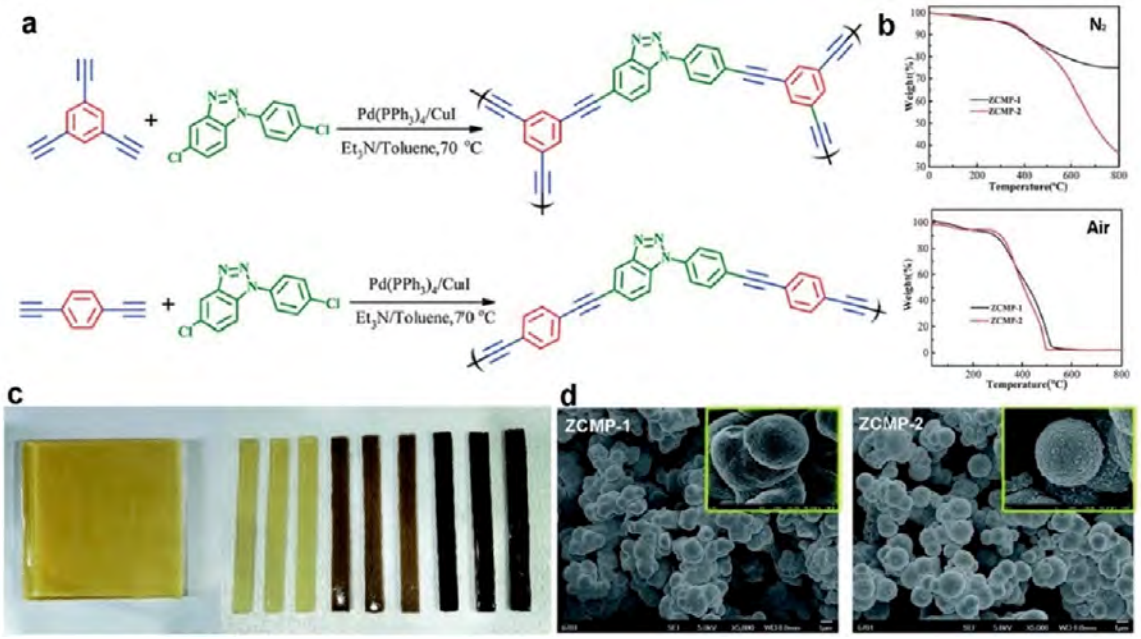

Figure 10. Benzotriazole-based conjugated microporous polymer gels with enhanced thermal insulation properties. (a) Synthesis of the ZCMPs. (b) TGA curves of ZCMPs under nitrogen and air. (c) Digital photograph of ZCMPs/EP composites. (d) SEM images and higher magnification images of ZCMP-1 (1,3,5-triethynylbenzene as the monomer) and ZCMP-2 (1,4-diethynylbenzene as the monomer). Scale bar: 1 μm, 100 nm. Reproduced with permission from ref 38. Copyright 2018 Royal Society of Chemistry.

100% (Figure 12c). In addition, the strain measurements (Figure 12d) and the rheological analysis (Figure 12e) showed that the CS/NH_2-TPP hydrogel could recover its original properties after dissociation.

Further, light microscope images (Figure 12f) proved the self-healing ability of micropores of the CS/NH_2-TPP hydrogel. When the hydrogel was cut into two pieces and then put together, the slits healed gradually over time, and the width of the slits decreased significantly after 15 min and healed completely after 30 min. For the macro level, when the hydrogel disk was drilled with a large hole (the diameter is one-third of the diameter of the disk), the pores completely disappeared and took on the appearance of the initial hydrogel disk after 30 min without external stimulation (Figure 12g). Through controlled experiments (Figure 12h), it can be observed that CS/NH_2-TPP self-healing hydrogels have better self-healing performance than normal hydrogels.

For application, The CS/NH_2-TPP hydrogel modified with folic acid (FA) can be used as a pH-sensitive, injectable, targeted drug delivery system.[101] If the strength and function of the CMP hydrogel are further enhanced and can be molded into any shape, it will be possible to form a gel with a more complex state for practical applications.

4. EXTENSIVE APPLICATION PROSPECT

This section mainly introduces the application prospect of CMP gels and monoliths, including drug delivery and wound healing, flame retardant and insulation, heterogeneous catalysis, clean water supply, gas storage, and sensors. As an illustration of this, some CMP gels are conjugated with components with specific biological functions to form hydrogel networks, which can effectively control their degradation rate and immune irritation in vivo.[77,101] Meanwhile, a CMP-based hydrogel nanofiber membrane synthesized by electrospinning can selectively kill pathogens under visible light while providing sustained protection to the wound.[76] As typical catalysts, CMP gels and monoliths with adjustable pore shape and size greatly facilitate the transport of matrix and catalytic products.[87,88,102] Furthermore, compared with CMP powders, CMP gels and monoliths have better recyclability and portability, improving their application value in the field of flame retardant, gas adsorption, and sensing.

4.1. Drug Delivery and Wound Healing. With the CMPs as a platform, the conjugated cross-linking of porphyrins into the CMP hydrogel network is an effective strategy to solve the two major challenges faced by porphyrins in the field of biomedical science, the lack of biocompatibility and cell selectivity. Belali et al. obtained a pH-sensitive and cancer-targeting photosensitizer carrier (CS/NH_2-TPP/FA) by conjugating cross-linking porphyrin groups into the CMP hydrogel network through a Schiff-base reaction and then surface modification with FA.[101] The microporous cross-linked structure can reduce the accumulation of porphyrin in the biological environment. The properties of hydrogels increase the biocompatibility of porphyrin-based drug, . and the conjugated cross-linked structure provides a more stable chemical structure to prevent the leaching of porphyrins in biological circulatory systems.

The microporous structure of CS/NH_2-TPP/FA effectively prevents the aggregation of porphyrin units and promotes energy transfer to improve the release of singlet oxygen. Compared with porphyrin alone (0.5), the CS/NH_2-TPP/FA showed a higher singlet oxygen quantum yield (0.64).[101] Meanwhile, the CS/NH_2-TPP/FA hydrogel with high biological compatibility and stability in biological circulatory systems showed high stability in biological medium (pH 7.4) and could release porphyrin-based photosensitizer rapidly and in large quantities in the physiological acidic condition (pH 5).[101] This is beneficial, as the CMP hydrogel provides a feasible way for building smart drug delivery hydrogel systems to advance anticancer technologies in a safer direction.

https://doi.org/10.1021/acsami.2c10088
ACS Appl. Mater. Interfaces 2022, 14, 39701−39726

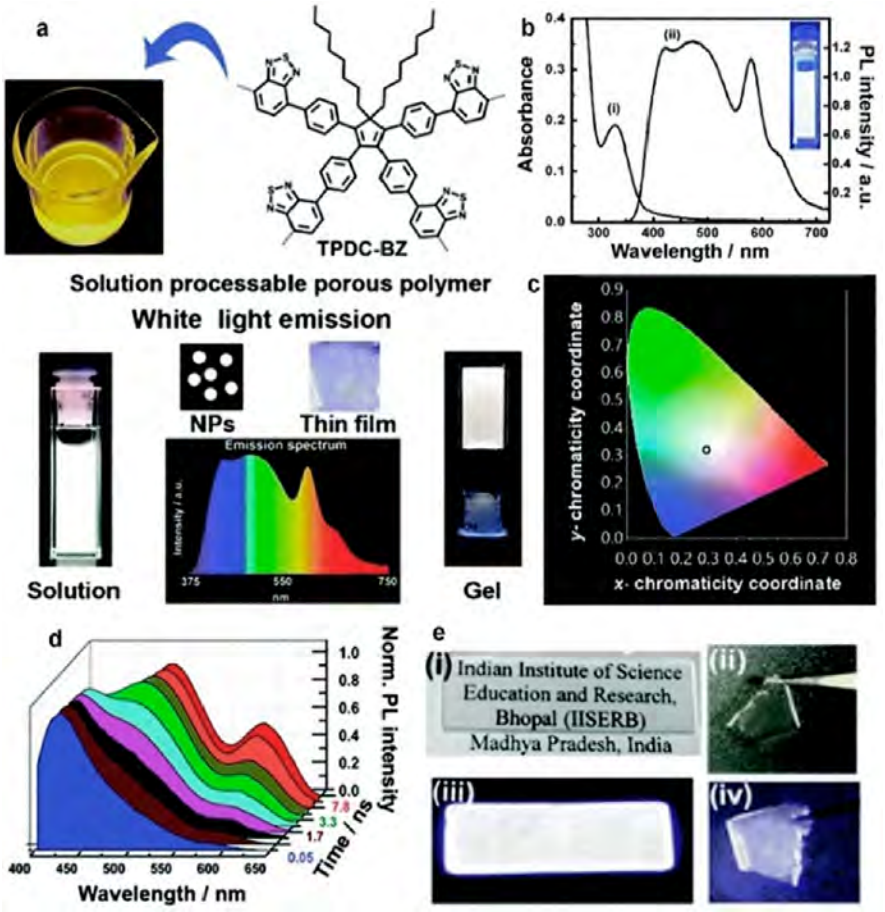

Figure 11. Processable conjugated porous organic polymer with efficient white light emission. (a) Schematic illustration depicting the versatile use of a strongly fluorescent and soluble TPDC−BZ for efficient white light emission. (b) Spectral characteristics of the WLE nanoparticle dispersion: (i) absorption and (ii) emission (λ_{ex} = 340 nm) spectra. Inset: photograph of WLE nanoparticles under irradiation at 365 nm. (c) Chromaticity diagram (CIE 1931) of the nanoparticles (x = 0.29, y = 0.32). (d) Time-resolved emission (TRES) spectra of an aqueous dispersion of nanoparticles with the wavelength range from 400 to 650 nm and delay time from 54 ps to 7.8 ns. (e) Photographs of (i) a transparent gel coated on a quartz plate and (ii) a free-standing thin film in daylight. (iii) Gel-coated quartz plate and (iv) thin-film exhibiting white light emission under UV light. Reproduced with permission from ref 45. Copyright 2017 Royal Society of Chemistry.

Modeled on human cells, FA-functionalized CMP hydrogels have excellent selectivity to kill cancer cells, with little damage to normal cells, due to the presence of FA contributing to recognizing cancer cells.[77,101] In 2020, Razzaque et al. reported the high biocompatibility of FA-functionalized hyper-cross-linked microporous organic polyethylene capsules (HMOCs-FA), which can recognize cancer cells and deliver anticancer drugs.[77] Pyrene units are added to the capsules to further enhance the fluorescent imaging, the pyrene-added HMOCs-FA aliased as Py-HMOCs-FA. As shown in Figure 13, the contrast agent (DAPI) used to locate the nucleus appears blue, while doxorubicin (DOX) emits red fluorescence. Compared with free DOX and DOX-loaded Py-HMOC (Py-HMOC/DOX), the DOX-loaded Py-HMOC-FA (Py-HMOC-FA/DOX) can transport DOX around the cancer cell nucleus more stably and accurately and release. This further confirms that the CMP hydrogel is a robust platform for the effective and selective delivery of anticancer drugs to cancerous tissues.

In addition, to replace traditional antibacterial wound dressings, Landfester et al. prepared a CMP-based hydrogel nanofibrous membrane for photocatalytic sterilization that provides continuous protection for a wound surface under visible light.[76] Preparation of the photoactive CMP-based wound dressings (Figure 14a) includes the first preparation of the photoactive benzo[c]-1,2,5-oxadiazole-based CMP nanoparticles (TBO NPs) by polymerization in microemulsion and then embedding TBO NPs into poly(vinyl alcohol) (PVA) hydrogel nanofibers via colloidal electrospinning. The CMP-based nanofibrous membrane (PVA-TBO nanofibrous membrane) has a highly cross-linked structure that prevents embedded TBO NPs from leaking into the wound, as well as outstanding mechanical robustness that prevents the nanofibrous membrane from being damaged during use.

For the *Escherichia coli* (*E. coli*) K-12 and *Bacillus subtilis* (*B. subtilis*) model system, the PVA-TBO nanofibrous membrane has outstanding disinfection performance under visible light. The PVA-TBO nanofibrous membrane could inactivate 100% *B. subtilis* and *E. coli* K-12 under visible light irradiation after 60 and 120 min of irradiation, respectively (Figure 14b), while pure PVA nanofibrous membrane cannot inactivate bacteria under light and PVA-TBO nanofibrous membrane cannot inactivate bacteria under dark conditions. The nanofibrous membrane allows for the insertion of other functional agents and growth factors, and the CMPs have functional adjustment properties, which together provide a powerful platform for the manufacture of multifunctional wound dressings. Furthermore,

https://doi.org/10.1021/acsami.2c10088
ACS Appl. Mater. Interfaces 2022, 14, 39701−39726

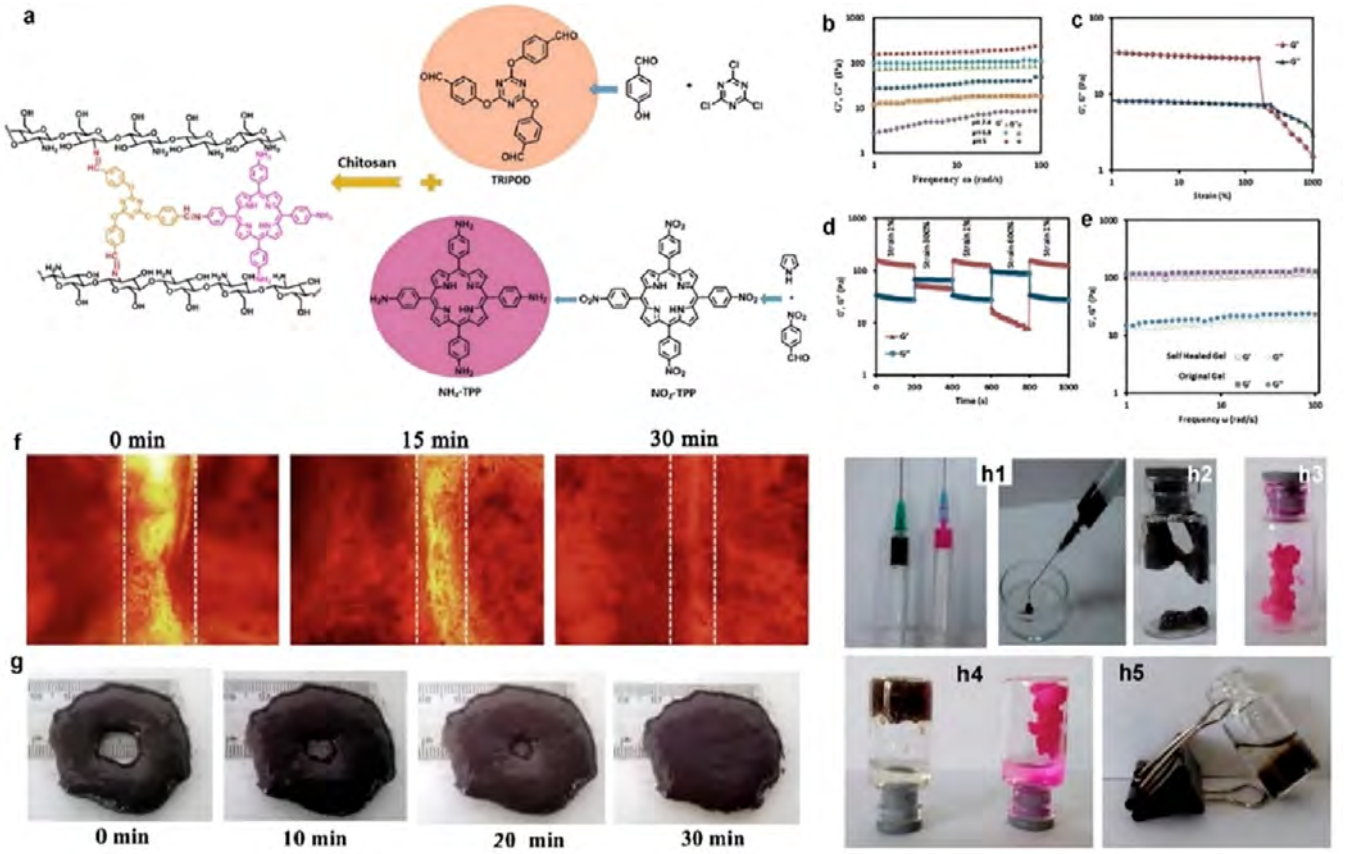

Figure 12. Conjugated microporous polymer-based chitosan hydrogel with self-healing property. (a) Chemical structures of preparation of CS/NH_2-TPP hydrogel. (b) Storage modulus (G') and loss modulus (G'') of CS/NH2-TPP hydrogel as functions of frequency at different pH values (hydrogels were immersed in buffers pH 7.4, 6.8, and 5.0 for 15 h before tests). (c) Damage-healing property of hydrogel demonstrated by the continuous step strain (1% strain → 300% strain → 1% strain → 600% strain → 1% strain) measurements. (d) G' and G'' of the hydrogel from strain amplitude sweep (λ = 1−1000%) at a fixed angular frequency (0.1 rad/s) and (e) G' and G'' of original and self-healed hydrogel. (f) Microscopic self-healing property of CS/NH_2-TPP hydrogel at neutral pH. (g) Macroscopic self-healing property of CS/NH_2-TPP hydrogel at 0−30 min. (h) Self-healing process after injection (dark purple, self-healing hydrogel; pink, gelatin hydrogel). Reproduced with permission from ref 101. Copyright 2018 Elsevier.

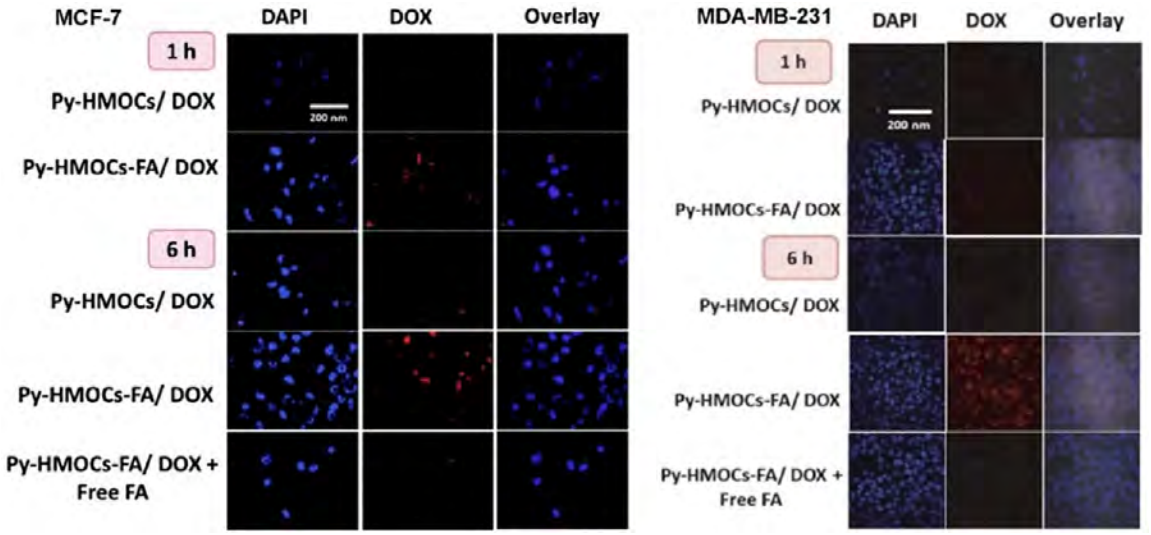

Figure 13. Functionalized hollow hyper-cross-linked microporous organic polyethylene capsules for doxorubicin delivery to cancer cells. Confocal microscopy images of DOX delivery to MCF-7 cell lines and MDA-MB-231 cell lines at different times by Py-HMOCs-DOX, Py-HMOCs-FA-DOX, and Py-HMOCs-FA-DOX + Free FA (scale bar = 200 nm). Reproduced with permission from ref 77. Copyright 2020 Royal Society of Chemistry.

https://doi.org/10.1021/acsami.2c10088
ACS Appl. Mater. Interfaces 2022, 14, 39701−39726

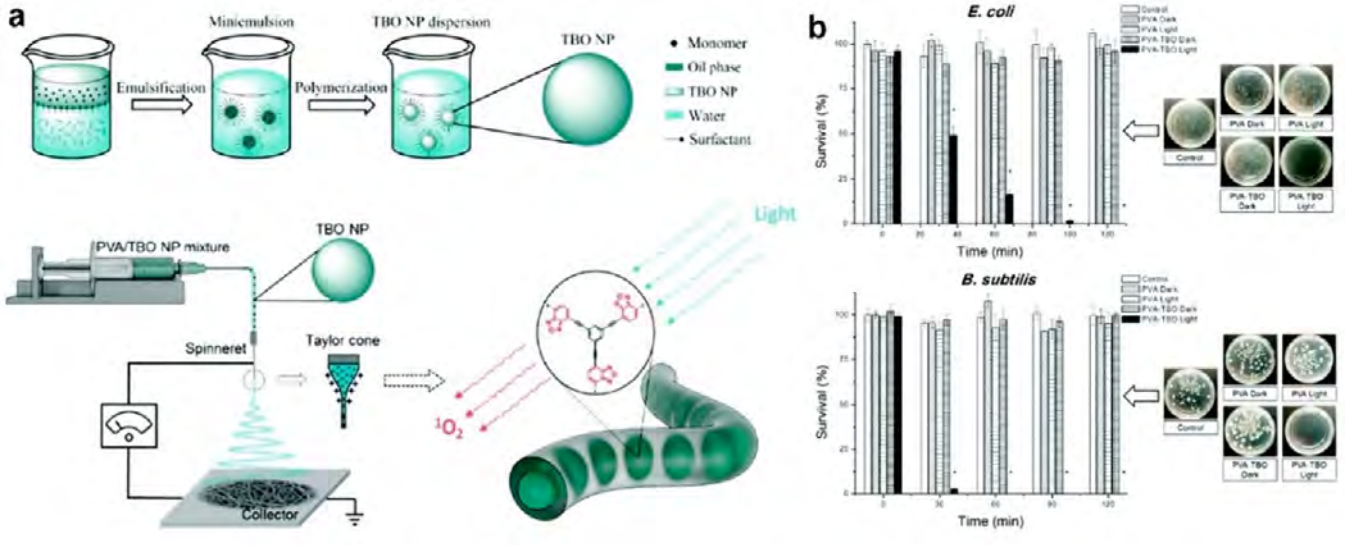

Figure 14. Conjugated microporous polymer gels as a platform for photocatalytic disinfection. (a) Schematic description of the fabrication process of the visible-light-active nanofibrous membrane: Synthesis of TBOs by miniemulsion polymerization and fabrication of PVA−TBO nanofibers by colloid electrospinning. (b) Photocatalytic inactivation of *E. coli* K-12 and *B. subtilis* in the presence of PVA and PVA−TBO membranes under dark conditions and visible light irradiation, as well as photographs of *E. coli* K-12 and *B. subtilis* colonies on an agar plate. Reproduced with permission from ref 76. Copyright 2018 Royal Society of Chemistry.

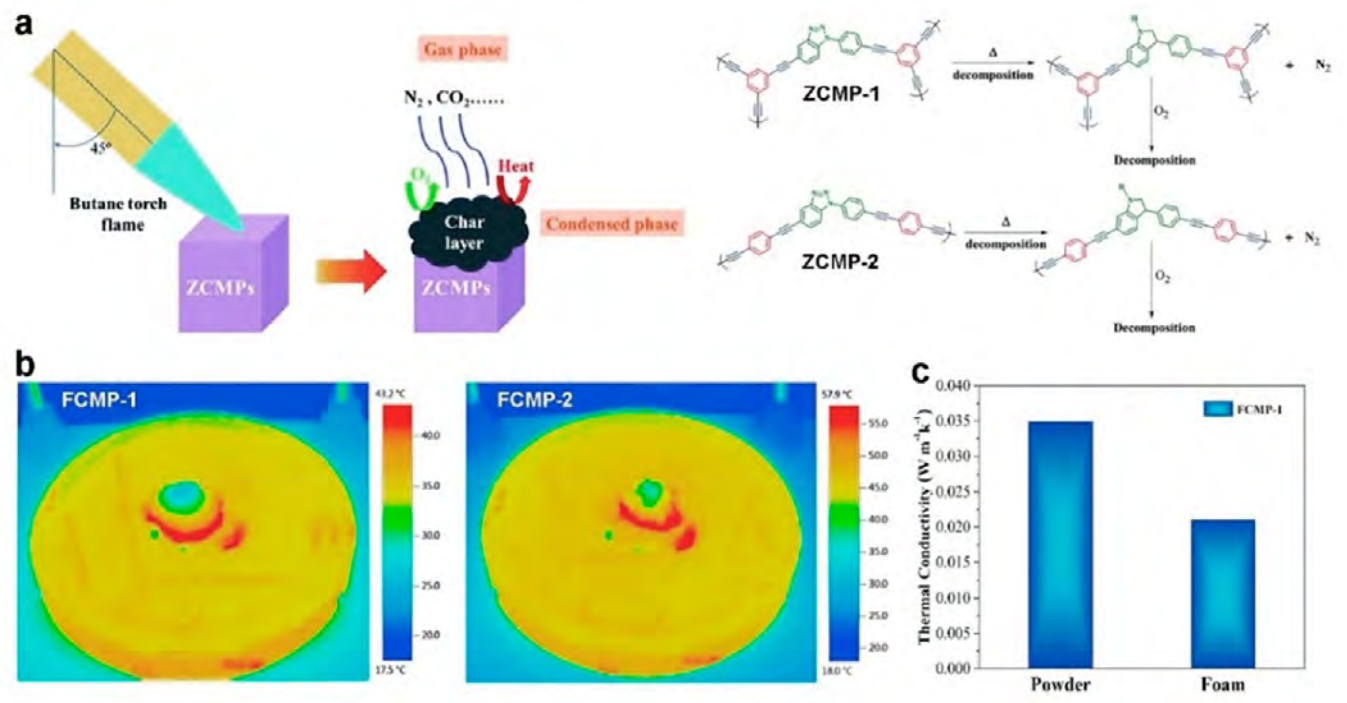

Figure 15. Conjugated microporous polymer monolithic nanofoams for flame retardant and insulation. (a) Schematic illustration of the flame-retardant mechanism of ZCMPs, and a possible mechanism for decomposition of ZCMP-1 and ZCMP-2. Reproduced with permission from ref 38. Copyright 2018 Royal Society of Chemistry. (b) Thermographic images of FCMP-1 and FCMP-2. (c) Thermal conductivity values of powdery FCMP-1 and FCMP-1 foam. Reproduced with permission from ref 103. Copyright 2018 Elsevier.

due to the limitations of the application conditions, the novel light-active CMP-based nanofibrous membrane is effective only for uncovered wound healing.

4.2. Flame Retardant and Insulation. The development of multifunctional green materials with low thermal conductivity and high flame-retardant performance is of great significance to the development of modern energy-saving buildings. With the advantages of high mechanical robustness, processability, and thermal stability, CMP monoliths have great potential to be used as new insulation materials in modern building construction.[38,103,104] In 2018, Li's group, as a pioneer, used the Sonogashira−Hagihara coupling reaction to reasonably design fluorine-rich CMP (FCMP) foams with heat insulation and flame retardant properties.[103] Compared with graphene oxide aerogel,[105] FCMP foams have comparable

https://doi.org/10.1021/acsami.2c10088
ACS Appl. Mater. Interfaces 2022, 14, 39701−39726

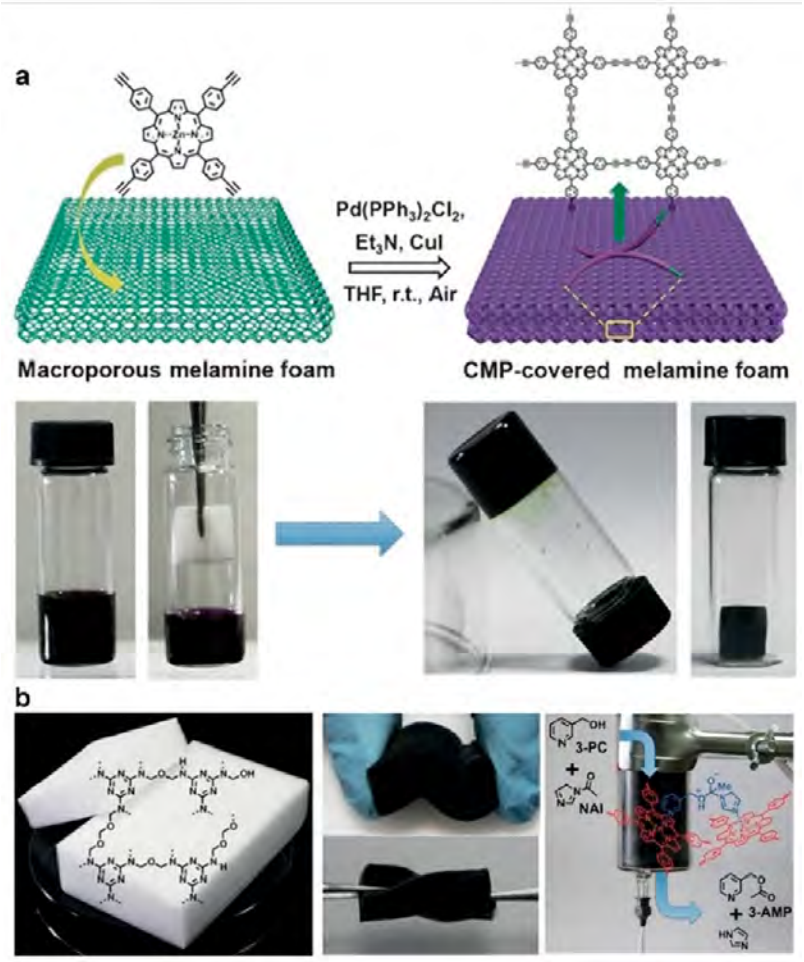

Figure 16. Elastic metalloporphyrin-containing conjugated microporous polymer monolith for process intensified acyl transfer. (a) CMP-gel-mediated composite strategy for the preparation of the CMP-covered foam composite; the synthetic procedure included mixing of the foam and reaction solution, gelation, solvent removal, and adhesion of CMPs to the foam. (b) Photographs of the melamine foam (left) and as-synthesized CMP foam composites (center). Representation of the acyl transfer reaction with a doubly bound intermediate in the micropore of ZnP-based frameworks (right, filling the glass syringe). Reproduced with permission from ref 87. Copyright 2016 Wiley−VCH.

thermal conductivity (0.021 W m^{-1} K^{-1}) and pHRR values (10.4−11.2 W g^{-1}).

The insulation mechanism of the system is mainly that the low density and thermal conductivity of CMP monoliths hinder heat conduction, as well as the limitation of hot air convection by micropores of CMP monoliths. Furthermore, the flame-retardant effect can be enhanced by introducing functional groups into CMP networks. Therefore, Li's group introduced the benzotriazole group into the CMP networks to prepare new benzotriazole-based CMP (ZCMP) composite monoliths that can produce a "green" gas (nitrogen) during combustion to enhance flame retardancy.[38] The flame retardant mechanism of ZCMP composite monoliths is shown in Figure 15a, where the surface of the CMP monoliths is degraded into carbon material to form a protective layer under high temperature; at the same time, nitrogen is generated during the degradation process to block oxygen and prevent the further destruction of ZCMP composite monoliths.

A thermal imaging test (Figure 15b) shows the surface temperature distribution of the FCMPs, which is often used to characterize the radiation transfer of the materials. Compared with FCMP-2 (1,4-diethynylbenzene as alkynyl monomer), the light blue part of FCMP-1 (1,3,5-triethynylbenzene as alkynyl monomer) in the thermal image test indicates that it has a better thermal insulation effect. Meanwhile, the thermal conductivity of FCMP-1 foam is lower than that of FCMP-1 powder (Figure 15c), so the FCMP-1 foam has better thermal insulation performance than FCMP-1 powder. The processed FCMP-1 foam has enhanced compression properties compared to the powdered CMPs, making it easier to embed into the wall as a flame-retardant material.

4.3. Heterogeneous Catalysis. Although CMPs have a highly stable conjugated porous structure and high density and accessible catalytic center,[106−110] diffusion in the microporous pores is easily inhibited in the presence of excessive reaction substrates. The hierarchical porous CMP foams have microporous pores and open channels, which can promote mass transfer, strengthen the catalytic process, and achieve the highest catalytic efficiency.[87,88,102] As shown in Figure 16a, the CMP monolith is formed by using melamine foam as the scaffold and a CMP organogel as the outer body, and the foam skeleton remains open to maintain elasticity and large channels. The hierarchical porous structure of the CMP-mediated foam facilitates the diffusion of the substrate in macropores and micropores, as well as is beneficial to the

https://doi.org/10.1021/acsami.2c10088
ACS Appl. Mater. Interfaces 2022, 14, 39701−39726

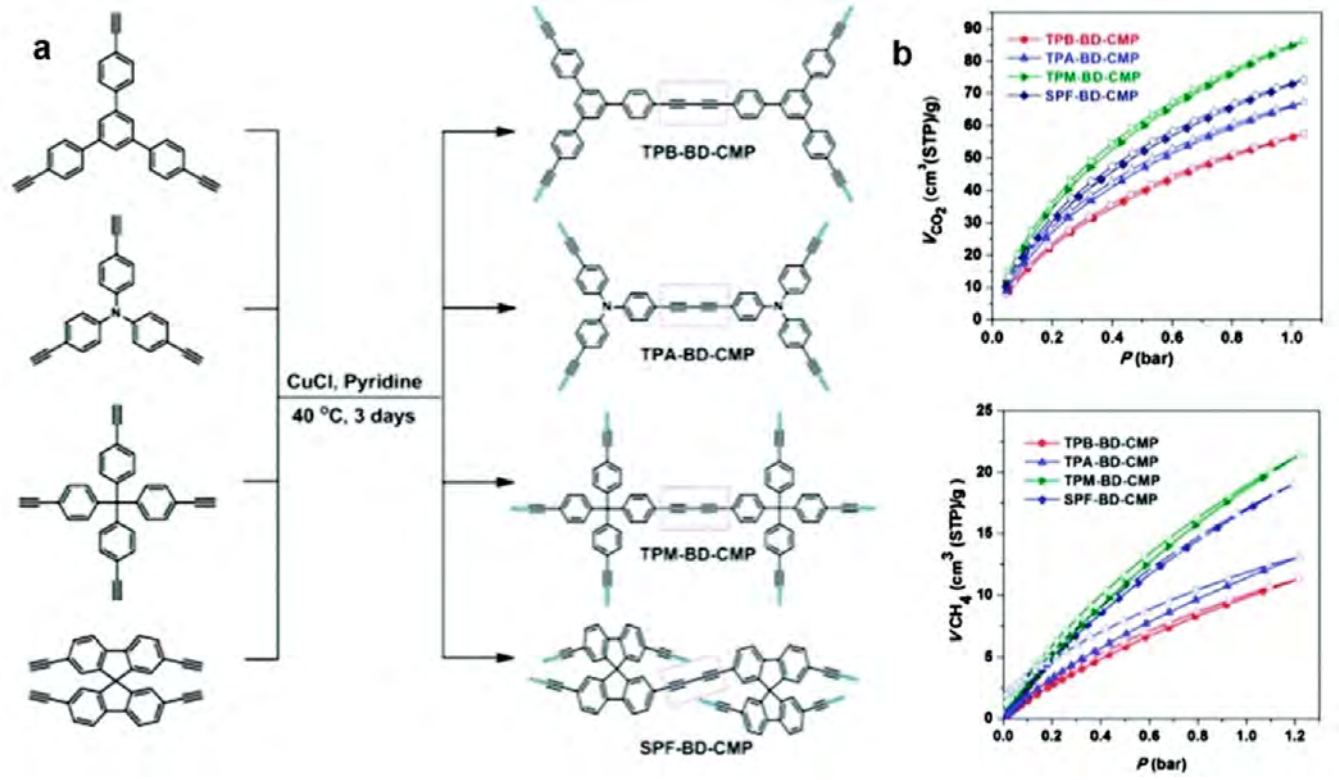

Figure 17. Butadiynylene-based conjugated porous polymer xerogels for CO_2 and CH_4 adsorption. (a) Synthetic routes for the four BD-CMPs, BD: butadiynylene. (b) Volumetric CO_2 and CH_4 sorption analysis for the four BDCMPs at 273 K (adsorption, filled symbols; and desorption, empty symbols). Reproduced with permission from ref 54. Copyright 2017 Royal Society of Chemistry and Chinese Chemical Society.

transfer of reaction products such as acyl groups (Figure 16b). Compared with the CMP powder,[29] the CMP-mediated foam has a higher product yield, although the specific surface area decreased.[87] This further indicates that both macroporous channels and microporous structures can improve the reaction rate.

From the practical effect, the loading efficiency of CMP solid adsorption on the foam surface or void is lower than expected.[87] Meanwhile, to develop a new generation of heterogeneous catalysts with good selectivity, high catalytic activity, and recoverability, it is usually necessary to introduce some special catalytic active sites. To illustrate, functionalized CMP monoliths serve as platforms to support uniformly dispersed noble metal nanoparticles with hierarchical porous structures and coordination environments within the structures, and to control fine-sized metal nanoparticles with adjustable functionalized monomers and appropriate reduction methods. In 2020, Tan et al. prepared CMP monoliths with different functions by changing the monomer ratio of 4-vinylpyridine (4VP) and styrene (St).[88] Due to the hierarchical porous structure and coordination environment, the prepared CMP monoliths provide abundant anchoring sites for metal precursors. Then sodium borohydride ($NaBH_4$) and the thermal reduction method can be used to reduce the metal precursors in the confined space to uniformly dispersed metal nanoparticles with fine particle size or even metal single atoms. For hydrogenation of 4-nitrophenol (4-NP), the CMP monolithic catalysts exhibit outstanding catalytic performance because of the hierarchical porous structure and abundant catalytic activity active sites. Meanwhile, the CMP monolithic catalysts have admirable catalytic stability. Among them, the Au@HCP-F-monolith-15 (15 denotes 15% monomer content of 4VP) can maintain high catalytic efficiency in five consecutive cycles and maintain the fine size of the metal catalytic center.

Introducing a sulfur site into the CMP foams, the structure loaded with Ag and the Ag-supported CMP foam catalysts could be obtained.[44] However, the loading effect of CMPs only changes its infiltration performance, which contributes little to the ultimate adsorption performance of the composite. Meanwhile, using the pure physical interaction composite in a harsh environment for a long time is difficult, which limits the further application of CMPs. In this regard, the introduction of noble metal catalytic sites into CMP monoliths through a polymerization reaction eliminates the noble metal loading process and produces stable chemical anchoring.[102] Due to the anchoring effect provided by the coordination groups of the CMP monolith and the confining effect provided by the micropores of the CMP monolith, fine and uniformly dispersed noble metal catalytic active sites are formed in molecular networks of the CMP monolith. The catalyst showed good activity in the low-temperature catalytic 4-NP reduction reaction and could keep the catalytic activity stable in a continuous flow state.

4.4. Gas Storage and Conversion. The CMP gels are one of the best organic porous polymers for gas storage due to the large specific surface area and outstanding gas affinity. In 2017, Chen et al. reported a convenient and efficient method (Figure 17a) for weaving a series of processable CMP xerogels with adjustable structures and properties.[54] All BD-CMPs formed stable physical gels in situ and were freeze-dried into xerogels. The BD-CMP xerogels have large specific surface areas (up to 1008 $m^2\ g^{-1}$), large total pore volumes (up to 1.11 $cm^3\ g^{-1}$), a hierarchical pore structure, and a fully extended π-

https://doi.org/10.1021/acsami.2c10088
ACS Appl. Mater. Interfaces 2022, 14, 39701−39726

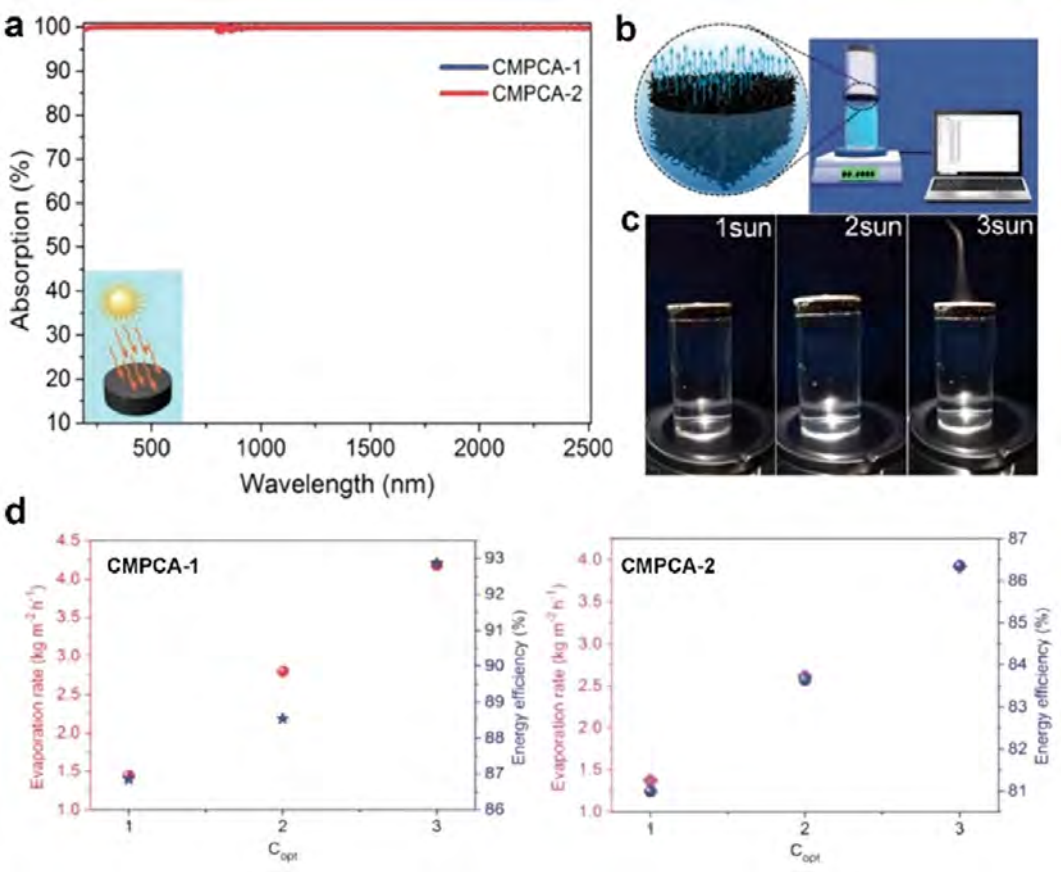

Figure 18. Conjugated microporous polymer gels derived hollow-carbon-nanotube aerogels for efficient solar steam generation. (a) UV−vis−NIR absorption spectra of the CMPCAs. Inset is a schematic diagram of solar energy absorption. (b) Schematic of solar steam generation. (c) Camera photos of steam generated under varied solar irradiation energy of 1-, 2-, and 3 kW m^{-2} (1−3 sun). (d) Evaporation rate (red, left-hand side axis) and solar steam efficiency (blue, right-hand side axis) of CMPCA-1 and CMPCA-2 under different illuminations. Reproduced with permission from ref 39. Copyright 2018 Wiley−VCH.

conjugate network. The CMP xerogels can be used for gas adsorption applications, and the CO_2 absorption capacity and CH_4 adsorption capacity are up to 3.78 and 0.95 mmol g^{-1}, respectively (Figure 17b). In general, with the increase in specific surface area, the amount of gas adsorption will also increase. However, compared with the non-nitrogenous CMP, the CMP with a nitrogenous skeleton has a higher gas affinity, which can compensate for the small specific surface area. As a illustration, although the specific surface area is smaller, TPA-BD-CMP (Figure 17b, blue line) has a larger gas capacity than TPB-BD-CMP (Figure 17b, red line).

The CMP gels not only have a hierarchical porous structure to capture CO_2 but also provide catalytic active sites to convert stored CO_2 into valuable chemicals to decrease CO_2 levels in the atmosphere. For instance, Zhang et al. developed a series of metalloporphyrin-based porous polymer gels (MTAPP-GO; M = Zn, Co, Pd; GO = glyoxal) using the dynamic covalent chemistry and postmodification strategies for the adsorption and chemical conversion of CO_2.[111] The obtained reticular gels have hierarchical porous structures, showing a strong affinity for CO_2 and the ability to capture a large amount of CO_2. Meanwhile, the CMP gels also have catalytic active sites to catalyze the heterogeneous cyclic addition of CO_2 and epoxides into cyclic carbonate. Among them, ZnTAPP-GO has the best catalytic performance and can be treated by the postmodification method to obtain ZnTAPP-GO-r with higher catalytic stability, which can be recycled at least five times.

The activity of the cycloaddition reaction of CO_2 and various epoxy substrates catalyzed by ZnTAPP-GO-r is related to the epoxy substrates.[111] Specifically, the conversion rate of various ZnTAPP-GO-r-catalyzed epoxy substrates to the corresponding cyclic carbonate is more than 88%, and the conversion rate of the CMP gel catalyzing the cycloaddition reaction of epoxypropyl phenyl ether is more than 99% in 10 h. Conversely, in the epoxidation of cyclohexane, the ZnTAPP-GO-r has only 34% conversion with low catalytic selectivity (45%). In the long term, the works provide a solution based on polymer chemistry and gel chemistry for the adsorption and chemical fixation of greenhouse gases.

4.5. Clean Water Supply. Solar steam generation has received a lot of attention in the field of clean water supply and is one of the most efficient ways to collect solar energy to produce freshwater. With the open channel structure, rich porosity and high specific surface area,[35] low thermal conductivity, and wide light absorption range,[112,113] CMP gels provide new openings for the design and manufacture of photothermal conversion materials with adjustable structure, adjustable porosity, and high solar conversion efficiency.[39,113] For instance, CMP aerogels composed of hollow nanotube wounds were synthesized by the monomer regulation method, and then new CMP carbon aerogels with high mechanical strength were obtained by simple carbonization. Meanwhile, CMPCAs were treated with a solution of sulfuric acid saturated with ammonium peroxysulfate to increase the superhydrophilic

https://doi.org/10.1021/acsami.2c10088
ACS Appl. Mater. Interfaces 2022, 14, 39701−39726

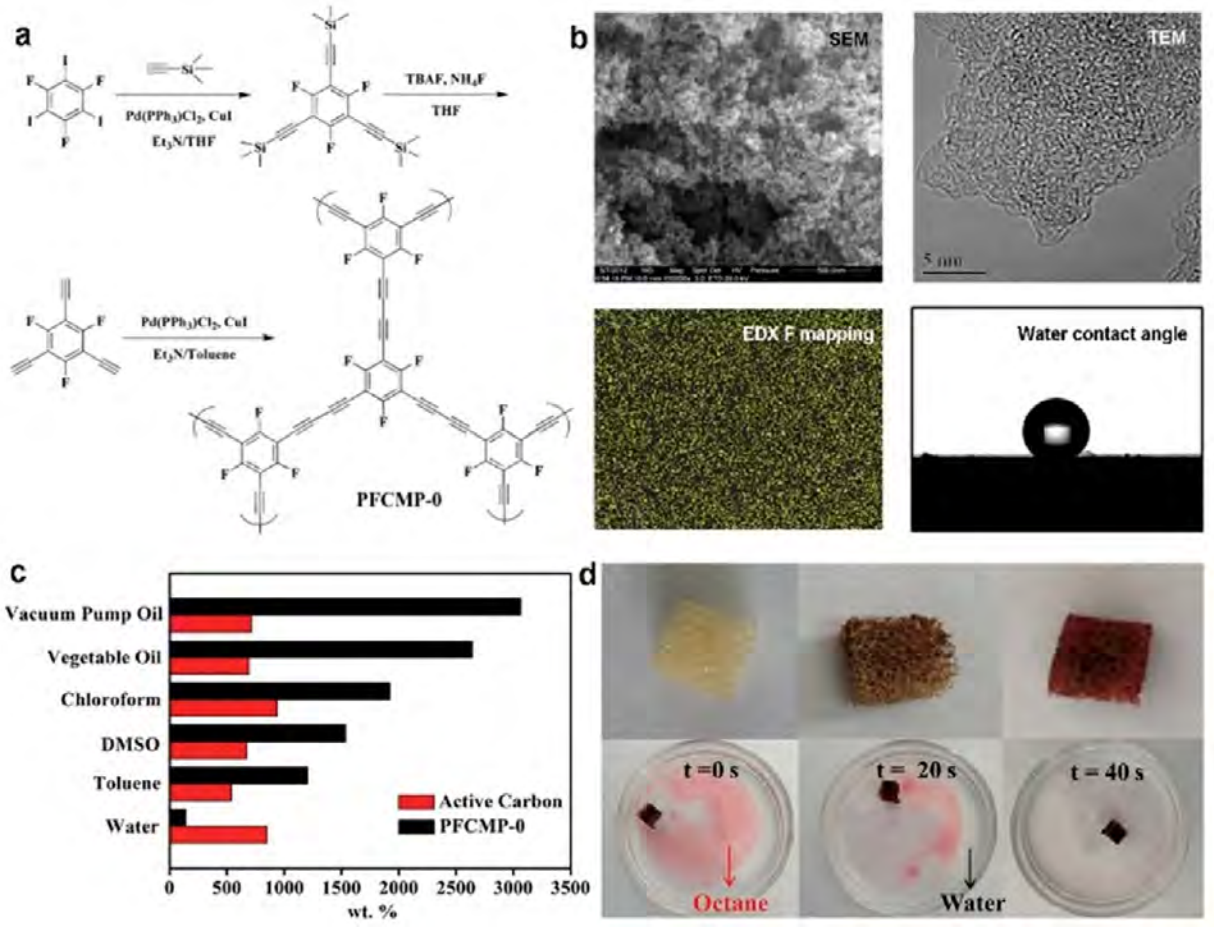

Figure 19. Superhydrophobic perfluorous conjugated microporous polymer monolith for solvents and oils adsorption. (a) Synthesis route of PFCMP-0. (b) SEM micrograph, corresponding EDX F mapping, HR-TEM micrograph, and the water contact angle of PFCMP-0. (c) Adsorption capacities of PFCMP-0 for different solvents and oils. (d) Top images from left to right are the untreated sponge ($0.6 \times 0.6 \times 0.6$ cm^3), the PFCMP-0 treated sponge before adsorption, and the treated sponge after adsorption; the bottom images display the octane (dyed by red oil) adsorption process. Reproduced with permission from ref 114. Available under a CC BY license.

wettability to speed up the transport of water molecules.[39] The CMPCAs retain composed of randomly aggregated hollow carbon nanotubes and form a hierarchical rigid network of nanopores after a series of treatments. Due to the porous structure, super hydrophilicity, low thermal conductivity, and excellent light absorption performance, the obtained CMPCAs can absorb almost 100% light in the range of 200−2500 nm (Figure 18a) for water evaporation. As shown in Figure 18a−d, the obtained CMPCAs are high performance in the field of solar steam generation, the evaporation rates reached up to 4.1778 and 3.9186 kg m^{-2} h^{-1} for CMPCA-1 and CMPCA-2, respectively. Furthermore, CMPCA-1 has a higher light energy conversion efficiency than CMPCA-2,[39] which could be due to the enhanced capillarity of CMPCA-1 micropores that can accelerate the transport of water molecules.

In addition, oil spills and industrial organic pollutants cause global water pollution, which seriously affects the clean water supply and the health of the ecological environment. Constructing effective adsorption materials for the removal of oil and organic pollutants from water relies on the unique properties of CMP gels, such as adjustable properties, hierarchical porosity, mechanical robustness, and chemical stability, is a constructive strategy to solve the global water environmental issues.[33] In 2011, Li et al. reported the first case of a superhydrophobic CMP sponge with excellent oil−water separation performance.[33] Because of the open pores and surface superhydrophobicity, the CMP sponge can easily adsorb and separate oil from water without absorbing water. Meanwhile, the superhydrophobic CMP sponge also has a high adsorption rate for polar organic pollutants and toxic pollutants, for instance, about 700−1500 wt % for HCMP-1 (synthesized by polymerization of 1,3,5-triethynylbenzene) sponge and about 600−2300 wt % for HCMP-2 (synthesized by polymerization of 1,3,5-triethynylbenzene and 1,4-diethynylbenzene) sponge.[33]

In 2015, Deng's group then reported a superhydrophobic perfluorous CMP (PFCMP-0), which was synthesized by homocoupling polymerization of 1,3,5-trifluoro-2,4,6-triethylbenzene (Figure 19a).[114] Field emission scanning electron microscopy (FE-SEM) image and high-resolution transmission electron microscopy (HR-TEM) image showed the PFCMP-0 network morphology and high microporosity, as well as the energy-dispersive X-ray spectrometer (EDX) analysis, showed that fluorine atoms replaced hydrogen atoms uniformly distributed in the PFCMP-0 network (Figure 19b). Compared with other CMPs, fluorine substitution provides PFCMP-0 with higher thermal stability (thermal decomposition temperature above 300 °C). Compared with commercial activated carbon, the PFCMP-0 treated sponge has an excellent adsorption capacity for oil, organic pollutants, and heavy

https://doi.org/10.1021/acsami.2c10088
ACS Appl. Mater. Interfaces 2022, 14, 39701−39726

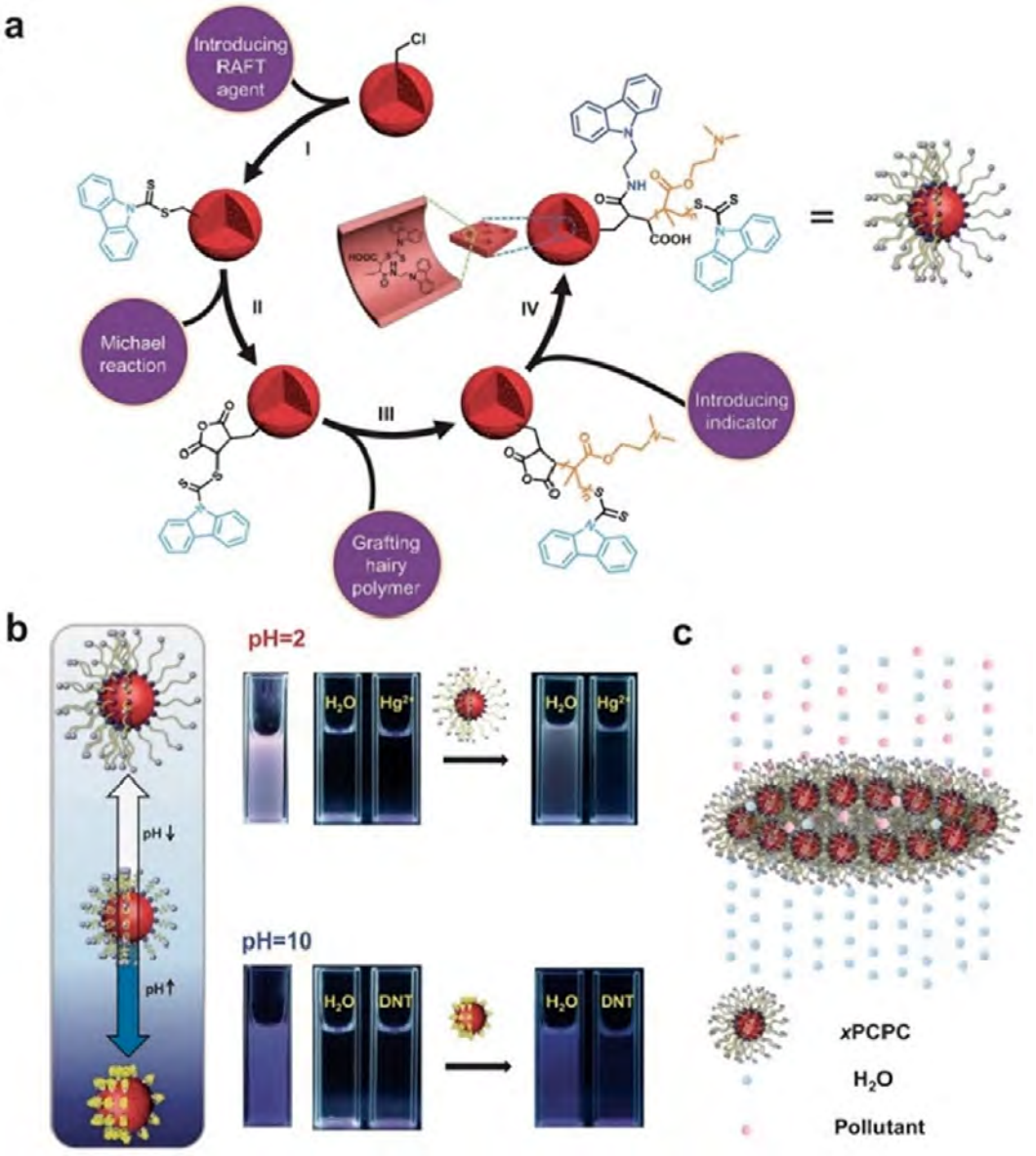

Figure 20. Intelligent conjugated microporous polymeric adsorbent materials with ultrafast adsorption of pollutants and response to environmental pollution. Schematic illustration for the (a) fabrication, (b) pH-response and pollutant-sensitive behavior, and (c) rapid contaminant removal performance of the all-in-one porous polymer adsorbent. Reproduced with permission from ref 115. Copyright 2019 Wiley−VCH.

metal ions (Figure 19c; 1200−3000 wt %) and rarely adsorbs water (Figure 19c; 142 wt %). Meanwhile, the PFCMP-0-treated sponge has a rapid absorption rate, completely removing the octane from the water in about 40 s (Figure 19d). Theoretical calculations showed that the outstanding properties of the PFCMP-0-treated sponge may be due to the internal fluorine substitution and continuous triple bond.

In 2017, Chang et al. prepared the compressible hierarchical porous CMP composites (PUS-MOP-A) by using 1,3,5-triethylbenzene, 1,4-diiodibenzene, and 2,5-diiodibenzoic acid as raw materials as well as polyurethane sponge (PUS).[53] Among them, PUS was used as a template to construct a compressible hierarchical porous skeleton, and 2,5-diiodobenzoic acid was used as a comonomer to provide a pH-sensitive pore surface. Meanwhile, adjusting the mole proportion of 1,4-diiodibenzene was used to form a fibrous micropore network in the porous channel of PUS-MOP-A. Finally, to adapt to the use in an aqueous environment, PUS-MOP-A was treated with KOH to convert the hydrophobic carboxyl group into a hydrophilic carboxylate anion to form a hydrophilic PUS-MOP-A (PUSU-MOP-Aa). The obtained PUSU-MOP-Aa can be used to assemble portable water purification devices for the rapid removal of methylene blue in the water. More interestingly, PUS-MOP-Aa also has selective adsorption properties, preferentially removing cationic dyes from water.

The CMP-based monoliths mentioned above have good selective adsorption performance and excellent stability for a variety of organic substances and oils, which have great potential for large-scale removal of toxic pollutants in water and solving environmental problems caused by marine oil spills. Currently, there are still many factors hindering the development of CMP gels and monoliths in the field of environmental adsorption, such as the slow absorption rate, which affects their application in rapid and continuous flow devices.

https://doi.org/10.1021/acsami.2c10088
ACS Appl. Mater. Interfaces 2022, 14, 39701−39726

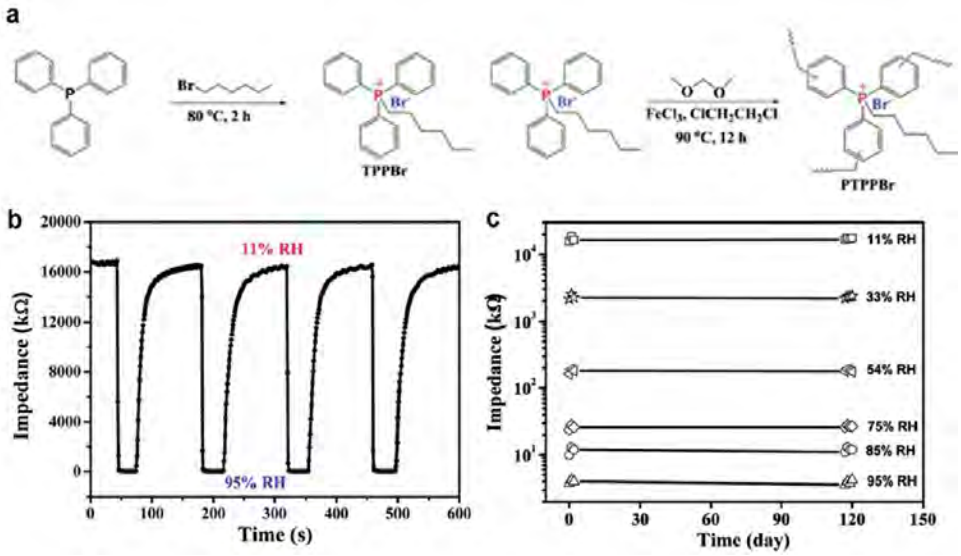

Figure 21. Humidity-sensitive conjugated microporous polymer gel with high sensitivity, rapid response recovery, and high stability. (a) Response and recovery curve of PTPPBr sensor between 11 and 95% RH (1 V AC, 100 Hz). (b) Stability of the PTPPBr sensor. Reproduced with permission from ref 120. Copyright 2014 Royal Society of Chemistry.

To treat pollutants more effectively from a complex environment, it is necessary to build intelligent CMP gels with ultrafast adsorption of pollutants, response to environmental pollution, and real-time monitoring capabilities. In this regard, Wu et al. developed a novel multifunctional CMP adsorption gel, the monodisperse hyper-cross-linked poly(4-chloromethylstyrene) nanosphere (*x*PCMS).[115] Then carbazole dithioester (Cz), maleic anhydride (MAh), and hairy poly(2-(dimethylamino)ethyl methacrylate) (PDMAEMA) were introduced into *x*PCMS step by step to obtain *x*PCMS-MAh/CEA-PDMAEMA-Cz (*x*PCPC; Figure 20a). The key to the successful design of the adsorbent is the synergy between the various functional components of the material. The high specific surface area and benzyl chloride groups of *x*PCMS provide high adsorption properties and functional graft sites. The surface-grafted PDMAEM can detect electron-sensitive aromatics and heavy metal ions due to the stretching/shrinking of the PDMAEM in acid/base conditions, resulting in visible pH-sensitive fluorescence changes (Figure 20b). Furthermore, the adsorbent has good adsorption performance in the high-speed flow adsorption test (Figure 20c). This work combines contaminant monitoring and adsorption to provide a solution for quickly detecting and removing contaminants from water, which points out a feasible direction for the construction of advanced smart CMP gels.

In developed countries and urban areas, the quality of drinking water is guaranteed thanks to powerful water purification plants and comprehensive pipe network distribution systems. However, in some developing countries and rural areas, the problem of water pollution has not been well solved. Diseases and deaths due to water pollution continue to threaten the inhabitants of these areas. In these areas, the investment cost of building centralized water purification and distribution systems is too high and there is a lack of existing facilities to support it. Improving the quality of drinking water in these areas will require a shift from traditional water purification models to ones that are low cost and easy to implement and maintain. The processable CMP gels and monoliths with water purification properties[116−118] provide viable technical support for modular water purification units for the small-scale treatment of specific water sources, such as household taps, community wells, and farm wastewater.

4.6. Humidity Sensors. Humidity-sensitive materials used as humidity sensors usually need to have a fine and stable structure and strong water resistance. Currently, the hydrophilic groups in amphiphilic polymer gels interact strongly with water molecules; especially, the condensation of dew after a long time of work can lead to the dissolution of the polymer gel, which makes the sensor lose high sensitivity and stability.[119] Therefore, a water-resistant polymer gel with a well-defined chemical structure is needed to ensure the stability of the humidity sensor under high humidity conditions.

The CMP gels have adjustable structure and performance and can be controlled by adjusting reaction conditions and monomer ratio,[3,18,32] which provides a feasible way the improvement of humidity-sensitive materials in humidity sensors. Zhang et al. synthesized the humidity-sensitive CMP gel (PTPPBr) by Friedel−Crafts reaction using triphenylphosphine as raw material (Figure 21a), which has a highly cross-linked skeleton structure, and the hydrophobic skeleton is uniformly modified by hydrophilic ions.[120] Many hydrophilic ions on the polymer skeleton rapidly interact with water molecules, the humidity-sensitive CMP gel (PTPPBr) provides high sensitivity, rapid response recovery, and small hysteresis (Figure 21b). Meanwhile, the highly cross-linked skeleton of the polymer provides excellent stability, maintaining sensor impedance stability for up to 120 days under different relative humidity conditions (Figure 21c). The CMP gel has outstanding sensing properties of high sensitivity, fast response recovery, insignificant humidity response hysteresis, and long-term impedance stabilization under high humidity conditions, which is of great significance for the practical application in humidity sensors.

In addition, smart polymers can respond to a variety of environments such as temperature, pH, and light stimuli,[121−124] which have received extensive attention in the field of sensors.[125−127] In an era of expanding population and

https://doi.org/10.1021/acsami.2c10088
ACS Appl. Mater. Interfaces 2022, 14, 39701−39726

increasing demand for food choices, food varieties are becoming more diverse and supply chains are becoming more global. To protect consumers from adulteration and fraud and to quickly identify contaminated food in response to global emergencies (such as outbreak management requirements), we need to develop more stable and responsive polymer materials that can be used to enhance sensor performance. Compared with ordinary smart polymer gels, the CMP gels have super cross-linked frameworks, which can maintain a high surface area and hierarchical porous structure in the dry state, which is incomparable to ordinary smart polymer gels. This is conducive to the design of a more stable and sensitive food detection sensor.

5. FUTURE PERSPECTIVES

In terms of construction, avoiding the formation of amorphous powder products is a prerequisite for the formation of generalized CMP gels and monoliths. In this review, we discuss in detail the basic formation routes of different CMP gels and monoliths. For example, the bottom-up processing[87] is flexibly applied to the composition between other CMP monomers and different support substrates. Compared to amorphous powders, the composite CMP gels and monoliths offer enhanced processability and mechanical robustness. However, the payload of the resulting final product by this method is limited. As well as the internal microporous of the CMP component could become blocked, reducing molecular accessibility.

Fortunately, the advantage of CMPs at the forefront of chemistry and material design lies in the unlimited monomer pairing and diverse synthetic pathways. Therefore, the structure and properties of CMPs can be finely adjusted to form pure CMP gels and monoliths with highly cross-linked structure, permanent microporous, and interpenetrating macropores by adjusting the monomer type and/or molar ratio as well as the reaction conditions. However, the formation mechanism of the synthetic pure CMP gels and monoliths is still poorly understood. Particularly, Accurate exploration of the interactions between nano-CMPs in the polymerization process is lacking. The systematic experimental verification and/or theoretical explanation of the intrinsic factors of the monomer molecule conversion into the final polymer is the basis for the further controlled synthesis of CMP gels and monoliths. Meanwhile, a finer understanding of these controlled internal parameters and the resulting controlled shaping process is conducive to reconstructing the existing CMP family for the preparation of pure CMP gels and monoliths.

In terms of properties and characterization, the CMP gels and monoliths retain the extended π-conjugated structure and high specific surface area of the original CMPs as well as the hierarchical porous structure of gels and monoliths. The bulk CMP gels and monoliths differ from amorphous powdered CMPs in that they also have enhanced ductility and processability. In this regard, the uniaxial and biaxial compression experiments can demonstrate the mechanical robustness of the CMP gels and monoliths under stress. Meanwhile, the bulk CMP gels and monoliths retain the thermostability of the original CMPs, and TGA can be used for thermostability evaluation to distinguish between bulk CMPs and ordinary bulk materials. Furthermore, if the CMP gels and monoliths respond to light radiation, combining some special spectroscopic analysis[45] is required to characterize the properties change during the light treatment. If the CMP gels and monoliths have self-healing, further information[101] on the rheology analyses, storage modulus and loss modulus, and morphology are also required.

In terms of potential applications, compared to other widely reported materials,[128−136] the multifunctional CMP gels and monoliths with careful design display promising prospects for widespread applications including gas separation, electrochromic devices, and energy storage.[81,137,138] Clinically, the injection of specific hydrogels into the body is an ideal method for drug delivery to target cells.[75,139−141] For this regard, the CMP gels serve as a powerful platform to conjugate components with specific biological functions into hydrogel networks and effectively control the release rate and immune irritation of vaccines.[75,77,142,143] For heterogeneous catalysis, with the help of powerful polymerization tools, different catalysis active molecules such as metalloporphyrin,[106,107,144,145] binol-derived phosphoric acid,[108,146] Tröger's base,[109,147] and N-heterocyclic carbene[110] can be introduced into the reconstructed 3D CMP conjugated networks for specific chemical applications. In addition, in the field of hydrogels and energy applications,[46,54,148−152] the CMP gels and monoliths with binding sites can tightly bind conductive materials for broad application prospects.

6. CONCLUSION

This review provides an objective analysis of the selected sample literature, elucidates the basic concepts, focuses on the construction methods and properties of the selected CMP gels and monoliths, and demonstrates the applications of the resulting gels and monoliths in drug delivery and wound healing, flame retardant and thermal insulation, heterogeneous photocatalysis, and sensing. As a finely modulated chemical platform, the diversity and versatility of the CMP monomer matrices in CMP gels and monoliths offer infinite options for regulating the application properties of processable polymer materials, including the appearance and shape. The 3D nanoscale cross-linking networks within the processable polymer translate molecular-scale information into material properties, offering interesting diverse properties and potential for widespread applications.

Theoretically, the existing amorphous powdery CMP family can be reconstructed with the construction principles and methods described in this review to produce processable CMP gels or monoliths with enhanced properties for device applications. Meanwhile, the newly designed CMPs can obtain ductility and processability by the gelation, providing new opportunities for the CMP family to solve energy and environmental issues. However, the field of CMP gels and monoliths is in its infancy. Compared to the conventional amorphous CMPs, the cause of CMP gel formation has never been systematically explained theoretically and verified experimentally, which is unfavorable to the controlled synthesis of CMP gel and monoliths. The subsequent work should make use of the diversity of monomer molecules in the CMP family to theoretically study the influence of molecular structure and activity on the formation mechanism of CMP gels and monoliths.

AUTHOR INFORMATION

Corresponding Authors

Guangming Zeng − *College of Environmental Science and Engineering, Hunan University and Key Laboratory of*

https://doi.org/10.1021/acsami.2c10088
ACS Appl. Mater. Interfaces 2022, 14, 39701−39726

Environmental Biology and Pollution Control (Ministry of Education), Hunan University, Changsha 410082, P.R. China; Center of Research Excellence in Renewable Energy and Power Systems, Center of Excellence in Desalination Technology, Department of Mechanical Engineering, Faculty of Engineering-Rabigh, King Abdulaziz University, Jeddah 21589, Saudi Arabia; orcid.org/0000-0002-4230-7647; Email: zgming@hnu.edu.cn

Zhifeng Liu − *College of Environmental Science and Engineering, Hunan University and Key Laboratory of Environmental Biology and Pollution Control (Ministry of Education), Hunan University, Changsha 410082, P.R. China; Center of Research Excellence in Renewable Energy and Power Systems, Center of Excellence in Desalination Technology, Department of Mechanical Engineering, Faculty of Engineering-Rabigh, King Abdulaziz University, Jeddah 21589, Saudi Arabia;* orcid.org/0000-0002-8598-4656; Email: zhifengliu@hnu.edu.cn

Authors

Songhao Luo − *College of Environmental Science and Engineering, Hunan University and Key Laboratory of Environmental Biology and Pollution Control (Ministry of Education), Hunan University, Changsha 410082, P.R. China; Center of Research Excellence in Renewable Energy and Power Systems, Center of Excellence in Desalination Technology, Department of Mechanical Engineering, Faculty of Engineering-Rabigh, King Abdulaziz University, Jeddah 21589, Saudi Arabia*

Eydhah Almatrafi − *Center of Research Excellence in Renewable Energy and Power Systems, Center of Excellence in Desalination Technology, Department of Mechanical Engineering, Faculty of Engineering-Rabigh, King Abdulaziz University, Jeddah 21589, Saudi Arabia*

Lin Tang − *College of Environmental Science and Engineering, Hunan University and Key Laboratory of Environmental Biology and Pollution Control (Ministry of Education), Hunan University, Changsha 410082, P.R. China; Center of Research Excellence in Renewable Energy and Power Systems, Center of Excellence in Desalination Technology, Department of Mechanical Engineering, Faculty of Engineering-Rabigh, King Abdulaziz University, Jeddah 21589, Saudi Arabia;* orcid.org/0000-0001-6996-7955

Biao Song − *College of Environmental Science and Engineering, Hunan University and Key Laboratory of Environmental Biology and Pollution Control (Ministry of Education), Hunan University, Changsha 410082, P.R. China; Center of Research Excellence in Renewable Energy and Power Systems, Center of Excellence in Desalination Technology, Department of Mechanical Engineering, Faculty of Engineering-Rabigh, King Abdulaziz University, Jeddah 21589, Saudi Arabia;* orcid.org/0000-0003-4390-650X

Chengyun Zhou − *College of Environmental Science and Engineering, Hunan University and Key Laboratory of Environmental Biology and Pollution Control (Ministry of Education), Hunan University, Changsha 410082, P.R. China; Center of Research Excellence in Renewable Energy and Power Systems, Center of Excellence in Desalination Technology, Department of Mechanical Engineering, Faculty of Engineering-Rabigh, King Abdulaziz University, Jeddah 21589, Saudi Arabia;* orcid.org/0000-0003-0948-0701

Yuxi Zeng − *College of Environmental Science and Engineering, Hunan University and Key Laboratory of Environmental Biology and Pollution Control (Ministry of Education), Hunan University, Changsha 410082, P.R. China; Center of Research Excellence in Renewable Energy and Power Systems, Center of Excellence in Desalination Technology, Department of Mechanical Engineering, Faculty of Engineering-Rabigh, King Abdulaziz University, Jeddah 21589, Saudi Arabia*

Complete contact information is available at: https://pubs.acs.org/10.1021/acsami.2c10088

Funding

The study was financially supported by the Program for Changjiang Scholars and Innovative Research Team in University (IRT-13R17), the National Natural Science Foundation of China (U20A20323, 51521006, 51378190, 51979103, 51679085, 51308200), the Fundamental Research Funds for the Central Universities of China (531107051205), the Funds of Hunan Science and Technology Innovation Project (2018RS3115), Natural Science Foundation of Hunan Province, China (2020JJ5069), the Key Research and Development Project of Hunan Province of China (2017SK2241), and the Three Gorges Follow-up Research Project (2017HXXY-05).

Notes

The authors declare no competing financial interest.

REFERENCES

(1) Jiang, J.-X.; Su, F.; Trewin, A.; Wood, C. D.; Campbell, N. L.; Niu, H.; Dickinson, C.; Ganin, A. Y.; Rosseinsky, M. J.; Khimyak, Y. Z.; Cooper, A. I. Conjugated microporous poly(aryleneethynylene) networks. *Angew. Chem., Int. Ed.* **2007**, *46* (45), 8574−8578.

(2) Dawson, R.; Laybourn, A.; Clowes, R.; Khimyak, Y. Z.; Adams, D. J.; Cooper, A. I. Functionalized Conjugated Microporous Polymers. *Macromolecules* **2009**, *42* (22), 8809−8816.

(3) Cooper, A. I. Conjugated microporous polymers. *Adv. Mater.* **2009**, *21* (12), 1291−1295.

(4) Jiang, J.-X.; Wang, C.; Laybourn, A.; Hasell, T.; Clowes, R.; Khimyak, Y. Z.; Xiao, J.; Higgins, S. J.; Adams, D. J.; Cooper, A. I. Metal-organic conjugated microporous polymers. *Angew. Chem., Int. Ed.* **2011**, *50* (5), 1072−1075.

(5) Xu, Y.; Jin, S.; Xu, H.; Nagai, A.; Jiang, D. Conjugated microporous polymers: design, synthesis and application. *Chem. Soc. Rev.* **2013**, *42* (20), 8012−8031.

(6) Hou, J.; Sapnik, A. F.; Bennett, T. D. Metal−organic framework gels and monoliths. *Chem. Sci.* **2020**, *11* (2), 310−323.

(7) Luo, S.; Zeng, Z.; Zeng, G.; Liu, Z.; Xiao, R.; Chen, M.; Tang, L.; Tang, W.; Lai, C.; Cheng, M.; Shao, B.; Liang, Q.; Wang, H.; Jiang, D. Metal organic frameworks as robust host of palladium nanoparticles in heterogeneous catalysis: Synthesis, application, and prospect. *ACS Appl. Mater. Interfaces* **2019**, *11* (36), 32579−32598.

(8) Liu, Y.; Cheng, H.; Cheng, M.; Liu, Z.; Huang, D.; Zhang, G.; Shao, B.; Liang, Q.; Luo, S.; Wu, T.; Xiao, S. The application of Zeolitic imidazolate frameworks (ZIFs) and their derivatives based materials for photocatalytic hydrogen evolution and pollutants treatment. *Chem. Eng. J.* **2021**, *417*, 127914.

(9) Liu, X.; Huang, D.; Lai, C.; Zeng, G.; Qin, L.; Wang, H.; Yi, H.; Li, B.; Liu, S.; Zhang, M.; Deng, R.; Fu, Y.; Li, L.; Xue, W.; Chen, S. Recent advances in covalent organic frameworks (COFs) as a smart sensing material. *Chem. Soc. Rev.* **2019**, *48* (20), 5266−5302.

(10) Wang, H.; Zeng, Z.; Xu, P.; Li, L.; Zeng, G.; Xiao, R.; Tang, Z.; Huang, D.; Tang, L.; Lai, C.; Jiang, D.; Liu, Y.; Yi, H.; Qin, L.; Ye, S.; Ren, X.; Tang, W. Recent progress in covalent organic framework thin films: fabrications, applications and perspectives. *Chem. Soc. Rev.* **2019**, *48* (2), 488−516.

(11) Wang, H.; Jiang, D.; Huang, D.; Zeng, G.; Xu, P.; Lai, C.; Chen, M.; Cheng, M.; Zhang, C.; Wang, Z. Covalent triazine frameworks for

carbon dioxide capture. *J. Mater. Chem. A* **2019**, *7* (40), 22848−22870.
(12) Martín-Illán, J. Á.; Rodríguez-San-Miguel, D.; Castillo, O.; Beobide, G.; Perez-Carvajal, J.; Imaz, I.; Maspoch, D.; Zamora, F. Macroscopic ultralight aerogel monoliths of imine-based covalent organic frameworks. *Angew. Chem., Int. Ed.* **2021**, *60* (25), 13969−13977.
(13) Sun, H.; Xu, Z.; Gao, C. Multifunctional, ultra-flyweight, synergistically assembled carbon aerogels. *Adv. Mater.* **2013**, *25* (18), 2554−2560.
(14) Feinle, A.; Elsaesser, M. S.; Hüsing, N. Sol−gel synthesis of monolithic materials with hierarchical porosity. *Chem. Soc. Rev.* **2016**, *45* (12), 3377−3399.
(15) Chivers, P. R. A.; Smith, D. K. Shaping and structuring supramolecular gels. *Nat. Rev. Mater.* **2019**, *4* (7), 463−478.
(16) Shang, T.; Lin, Z.; Qi, C.; Liu, X.; Li, P.; Tao, Y.; Wu, Z.; Li, D.; Simon, P.; Yang, Q.-H. 3D macroscopic architectures from self-assembled mxene hydrogels. *Adv. Funct. Mater.* **2019**, *29* (33), 1903960.
(17) Luo, S.; Zeng, Z.; Zeng, G.; Liu, Z.; Xiao, R.; Xu, P.; Wang, H.; Huang, D.; Liu, Y.; Shao, B.; Liang, Q.; Wang, D.; He, Q.; Qin, L.; Fu, Y. Recent advances in conjugated microporous polymers for photocatalysis: designs, applications, and prospects. *J. Mater. Chem. A* **2020**, *8* (14), 6434−6470.
(18) Luo, S.; Zeng, Z.; Wang, H.; Xiong, W.; Song, B.; Zhou, C.; Duan, A.; Tan, X.; He, Q.; Zeng, G.; Liu, Z.; Xiao, R. Recent progress in conjugated microporous polymers for clean energy: Synthesis, modification, computer simulations, and applications. *Prog. Polym. Sci.* **2021**, *115*, 101374.
(19) Slater, A. G.; Cooper, A. I. Function-led design of new porous materials. *Science* **2015**, *348* (6238), aaa8075.
(20) Zhang, X.; Lu, J.; Zhang, J. Porosity enhancement of carbazolic porous organic frameworks using dendritic building blocks for gas storage and separation. *Chem. Mater.* **2014**, *26* (13), 4023−4029.
(21) Broicher, C.; Foit, S. R.; Rose, M.; Hausoul, P. J. C.; Palkovits, R. A bipyridine-based conjugated microporous polymer for the ir-catalyzed dehydrogenation of formic acid. *ACS Catal.* **2017**, *7* (12), 8413−8419.
(22) Sprick, R. S.; Jiang, J. X.; Bonillo, B.; Ren, S.; Ratvijitvech, T.; Guiglion, P.; Zwijnenburg, M. A.; Adams, D. J.; Cooper, A. I. Tunable organic photocatalysts for visible-light-driven hydrogen evolution. *J. Am. Chem. Soc.* **2015**, *137* (9), 3265−3270.
(23) Zhang, H.; Zhang, Y.; Gu, C.; Ma, Y. Electropolymerized conjugated microporous poly(zinc-porphyrin) films as potential electrode materials in supercapacitors. *Adv. Energy Mater.* **2015**, *5* (10), 1402175.
(24) Wu, K.; Guo, J.; Wang, C. Dispersible and discrete metalloporphyrin-based CMP nanoparticles enabling colorimetric detection and quantitation of gaseous SO2. *Chem. Commun.* **2014**, *50* (6), 695−697.
(25) Hasell, T.; Cooper, A. I. Porous organic cages: soluble, modular and molecular pores. *Nat. Rev. Mater.* **2016**, *1* (9), 16053.
(26) Zhang, Y.-Z.; El-Demellawi, J. K.; Jiang, Q.; Ge, G.; Liang, H.; Lee, K.; Dong, X.; Alshareef, H. N. MXene hydrogels: fundamentals and applications. *Chem. Soc. Rev.* **2020**, *49* (20), 7229−7251.
(27) Cheng, G.; Hasell, T.; Trewin, A.; Adams, D. J.; Cooper, A. I. Soluble conjugated microporous polymers. *Angew. Chem., Int. Ed.* **2012**, *51* (51), 12727−12731.
(28) Zhang, P.; Weng, Z.; Guo, J.; Wang, C. Solution-dispersible, colloidal, conjugated porous polymer networks with entrapped palladium nanocrystals for heterogeneous catalysis of the Suzuki−Miyaura coupling reaction. *Chem. Mater.* **2011**, *23* (23), 5243−5249.
(29) Wu, K.; Guo, J.; Wang, C. Gelation of metalloporphyrin-based conjugated microporous polymers by oxidative homocoupling of terminal alkynes. *Chem. Mater.* **2014**, *26* (21), 6241−6250.
(30) Gu, C.; Chen, Y.; Zhang, Z.; Xue, S.; Sun, S.; Zhang, K.; Zhong, C.; Zhang, H.; Pan, Y.; Lv, Y.; Yang, Y.; Li, F.; Zhang, S.; Huang, F.; Ma, Y. Electrochemical route to fabricate film-like conjugated microporous polymers and application for organic electronics. *Adv. Mater.* **2013**, *25* (25), 3443−3448.
(31) Gu, C.; Huang, N.; Gao, J.; Xu, F.; Xu, Y.; Jiang, D. Controlled synthesis of conjugated microporous polymer films: Versatile platforms for highly sensitive and label-free chemo- and biosensing. *Angew. Chem., Int. Ed.* **2014**, *53* (19), 4850−4855.
(32) Gu, C.; Huang, N.; Chen, Y.; Qin, L.; Xu, H.; Zhang, S.; Li, F.; Ma, Y.; Jiang, D. π-Conjugated microporous polymer films: Designed synthesis, conducting properties, and photoenergy conversions. *Angew. Chem., Int. Ed.* **2015**, *54* (46), 13594−13598.
(33) Li, A.; Sun, H.-X.; Tan, D.-Z.; Fan, W.-J.; Wen, S.-H.; Qing, X.-J.; Li, G.-X.; Li, S.-Y.; Deng, W.-Q. Superhydrophobic conjugated microporous polymers for separation and adsorption. *Energy Environ. Sci.* **2011**, *4* (6), 2062−2065.
(34) Du, R.; Zhang, N.; Xu, H.; Mao, N.; Duan, W.; Wang, J.; Zhao, Q.; Liu, Z.; Zhang, J. CMP aerogels: Ultrahigh-surface-area carbon-based monolithic materials with superb sorption performance. *Adv. Mater.* **2014**, *26* (47), 8053−8058.
(35) Chen, Y.; Sun, H.; Yang, R.; Wang, T.; Pei, C.; Xiang, Z.; Zhu, Z.; Liang, W.; Li, A.; Deng, W. Synthesis of conjugated microporous polymer nanotubes with large surface areas as absorbents for iodine and CO2 uptake. *J. Mater. Chem. A* **2015**, *3* (1), 87−91.
(36) Mu, P.; Sun, H.; Zhu, Z.; He, J.; Liang, W.; Li, A. Monolithic nanofoam based on conjugated microporous polymer nanotubes with ultrahigh mechanical strength and flexibility for energy storage. *J. Mater. Chem. A* **2018**, *6* (25), 11676−11681.
(37) Liao, Y.; Wang, H.; Zhu, M.; Thomas, A. Efficient supercapacitor energy storage using conjugated microporous polymer networks synthesized from Buchwald−Hartwig coupling. *Adv. Mater.* **2018**, *30* (12), 1705710.
(38) Wei, H.; Wang, F.; Sun, H.; Zhu, Z.; Xiao, C.; Liang, W.; Yang, B.; Chen, L.; Li, A. Benzotriazole-based conjugated microporous polymers as efficient flame retardants with better thermal insulation properties. *J. Mater. Chem. A* **2018**, *6* (18), 8633−8642.
(39) Mu, P.; Zhang, Z.; Bai, W.; He, J.; Sun, H.; Zhu, Z.; Liang, W.; Li, A. Superwetting monolithic hollow-carbon-nanotubes aerogels with hierarchically nanoporous structure for efficient solar steam generation. *Adv. Energy Mater.* **2019**, *9* (1), 1802158.
(40) Jeong, S.; Chae, J. A.; Kim, H. J.; Jung, D.; Kim, Y. A.; Choi, E.; Kim, H. Hierarchical design of functional, fibrous, and microporous polymer monoliths for the molecular recognition of diethylstilbestrol. *Anal. Chem.* **2021**, *93* (40), 13513−13519.
(41) Yang, X.; Tan, L.; Xia, L.; Wood, C. D.; Tan, B. Hierarchical porous polystyrene monoliths from PolyHIPE. *Macromol. Rapid Commun.* **2015**, *36* (17), 1553−1558.
(42) Bao, L.; Sun, H.; Zhu, Z.; Liang, W.; Mu, P.; Zang, J.; Li, A. Synthesis and properties of tubular-shape conjugated microporous polymers with high purity. *Mater. Lett.* **2016**, *178*, 5−9.
(43) Kim, J. G.; Choi, T. J.; Chang, J. Y. Homogenized electrospun nanofiber reinforced microporous polymer sponge. *Chem. Eng. J.* **2016**, *306*, 242−250.
(44) Kim, J. G.; Cha, M. C.; Lee, J.; Choi, T.; Chang, J. Y. Preparation of a sulfur-functionalized microporous polymer sponge and in situ growth of silver nanoparticles: A compressible monolithic catalyst. *ACS Appl. Mater. Interfaces* **2017**, *9* (43), 38081−38088.
(45) Pallavi, P.; Bandyopadhyay, S.; Louis, J.; Deshmukh, A.; Patra, A. A soluble conjugated porous organic polymer: efficient white light emission in solution, nanoparticles, gel and transparent thin film. *Chem. Commun.* **2017**, *53* (7), 1257−1260.
(46) Lyu, W.; Zhang, W.; Liu, H.; Liu, Y.; Zuo, H.; Yan, C.; Faul, C. F. J.; Thomas, A.; Zhu, M.; Liao, Y. Conjugated microporous polymer network grafted carbon nanotube fibers with tunable redox activity for efficient flexible wearable energy storage. *Chem. Mater.* **2020**, *32* (19), 8276−8285.
(47) Vilela, F.; Zhang, K.; Antonietti, M. Conjugated porous polymers for energy applications. *Energy Environ. Sci.* **2012**, *5* (7), 7819−7832.
(48) Lee, J.-S. M.; Cooper, A. I. Advances in conjugated microporous polymers. *Chem. Rev.* **2020**, *120* (4), 2171−2214.

https://doi.org/10.1021/acsami.2c10088
ACS Appl. Mater. Interfaces 2022, 14, 39701−39726

(49) Taylor, D.; Dalgarno, S. J.; Xu, Z.; Vilela, F. Conjugated porous polymers: incredibly versatile materials with far-reaching applications. *Chem. Soc. Rev.* **2020**, *49* (12), 3981−4042.
(50) Zhang, W.; Zuo, H.; Cheng, Z.; Shi, Y.; Guo, Z.; Meng, N.; Thomas, A.; Liao, Y. Macroscale conjugated microporous polymers: Controlling versatile functionalities over several dimensions. *Adv. Mater.* **2022**, *34*, 2104952.
(51) Du, R.; Zheng, Z.; Mao, N.; Zhang, N.; Hu, W.; Zhang, J. Fluorosurfactants-directed preparation of homogeneous and hierarchical-porosity CMP aerogels for gas sorption and oil cleanup. *Adv. Sci.* **2015**, *2* (1−2), 1400006.
(52) Fan, W.; Liu, X.; Zhang, Z.; Zhang, Q.; Ma, W.; Tan, D.; Li, A. Conjugated microporous polymer nanotubes and hydrophobic sponges. *Microporous Mesoporous Mater.* **2014**, *196*, 335−340.
(53) Choi, T. J.; Kim, D. Y.; Chang, J. Y. Water wettable, compressible, and hierarchically porous polymer composite. *Microporous Mesoporous Mater.* **2017**, *242*, 82−89.
(54) Xie, Z.; Wei, Y.; Zhao, X.; Li, Y.; Ding, S.; Chen, L. Facile construction of butadiynylene based conjugated porous polymers by cost-effective Glaser coupling. *Mater. Chem. Front* **2017**, *1* (5), 867−872.
(55) Jia, P.; Hu, T.; He, Q.; Cao, X.; Ma, J.; Fan, J.; Chen, Q.; Ding, Y.; Pyun, J.; Geng, J. Synthesis of a macroporous conjugated polymer framework: Iron doping for highly stable, highly efficient lithium sulfur-batteries. *ACS Appl. Mater. Interfaces* **2019**, *11* (3), 3087−3097.
(56) Zhu, Z.; Wei, H.; Wang, F.; Sun, H.; Liang, W.; Li, A. Ionic liquid-based monolithic porous polymers as efficient flame retardant and thermal insulation materials. *Polymer* **2019**, *185*, 121947.
(57) Kim, B. S.-I.; Jin, Y.-J.; Sakaguchi, T.; Lee, W.-E.; Kwak, G. Fluorescence response of conjugated polyelectrolyte in an immiscible two-phase system via nonelectrostatic interaction with surfactants. *ACS Appl. Mater. Interfaces* **2015**, *7* (24), 13701−13706.
(58) Mohamed, M. G.; Zhang, X.; Mansoure, T. H.; El-Mahdy, A. F. M.; Huang, C.-F.; Danko, M.; Xin, Z.; Kuo, S.-W. Hypercrosslinked porous organic polymers based on tetraphenylanthraquinone for CO2 uptake and high-performance supercapacitor. *Polymer* **2020**, *205*, 205.
(59) Zheng, M.; Huang, H.; Jiang, Z.; Zhao, Y.; Sun, Y.; Zhong, C. Superhydrophobic conjugated porous organic polymer coated polyurethane sponge for efficient oil/water separation. *J. Porous Mater.* **2022**, *29* (2), 433−444.
(60) Lim, Y.; Cha, M. C.; Chang, J. Y. Compressible and monolithic microporous polymer sponges prepared via one-pot synthesis. *Sci. Rep.* **2015**, *5* (1), 15957.
(61) Preis, E.; Widling, C.; Scherf, U.; Patil, S.; Brunklaus, G.; Schmidt, J.; Thomas, A. Aromatic, microporous polymer networks with high surface area generated in Friedel−Crafts-type polycondensations. *Polym. Chem.* **2011**, *2* (10), 2186−2189.
(62) Yuan, K.; Guo-Wang, P.; Hu, T.; Shi, L.; Zeng, R.; Forster, M.; Pichler, T.; Chen, Y.; Scherf, U. Nanofibrous and graphene-templated conjugated microporous polymer materials for flexible chemosensors and supercapacitors. *Chem. Mater.* **2015**, *27* (21), 7403−7411.
(63) Lee, J. J.; Noh, W.; Huh, T.-H.; Kwark, Y.-J.; Lee, T. S. Synthesis of conjugated microporous polymer and its embedding in porous nanofibers for visible-light-driven photocatalysis with reusability. *Polymer* **2020**, *211*, 123060.
(64) Jing, B.; Lei, T.; Wang, J.; Xu, L.; Liu, J.; Sun, H.; Gao, S.; Miao, F.; Zang, Y. Synthesis of fluorine-containing conjugated microporous polymers and their application for highly efficient oil/water separation. *Microporous Mesoporous Mater.* **2022**, *339*, 111990.
(65) Nelson, A. P.; Farha, O. K.; Mulfort, K. L.; Hupp, J. T. Supercritical processing as a route to high internal surface areas and permanent microporosity in metal−organic framework materials. *J. Am. Chem. Soc.* **2009**, *131* (2), 458−460.
(66) Zhang, H.; Hussain, I.; Brust, M.; Butler, M. F.; Rannard, S. P.; Cooper, A. I. Aligned two- and three-dimensional structures by directional freezing of polymers and nanoparticles. *Nat. Mater.* **2005**, *4* (10), 787−793.
(67) Li, A.; Lu, R.-F.; Wang, Y.; Wang, X.; Han, K.-L.; Deng, W.-Q. Lithium-doped conjugated microporous polymers for reversible hydrogen storage. *Angew. Chem., Int. Ed.* **2010**, *49* (19), 3330−3333.
(68) Jiang, J.-X.; Su, F.; Niu, H.; Wood, C. D.; Campbell, N. L.; Khimyak, Y. Z.; Cooper, A. I. Conjugated microporous poly(phenylene butadiynylene)s. *Chem. Commun.* **2008**, No. 4, 486−488.
(69) Arab, P.; Rabbani, M. G.; Sekizkardes, A. K.; İslamoğlu, T.; El-Kaderi, H. M. Copper(I)-catalyzed synthesis of nanoporous azo-linked polymers: Impact of textural properties on gas storage and selective carbon dioxide capture. *Chem. Mater.* **2014**, *26* (3), 1385−1392.
(70) Kuhn, P.; Antonietti, M.; Thomas, A. Porous, covalent triazine-based frameworks prepared by ionothermal synthesis. *Angew. Chem., Int. Ed.* **2008**, *47* (18), 3450−3453.
(71) Lee, J.; Chang, J. Y. Preparation of a compressible and hierarchically porous polyimide sponge via the sol-gel process of an aliphatic tetracarboxylic dianhydride and an aromatic triamine. *Chem. Commun.* **2016**, *52* (68), 10419−10422.
(72) Zhu, Z.; Mu, P.; Fan, Y.; Bai, W.; Zhang, Z.; Sun, H.; Liang, W.; Li, A. Highly efficient solar steam generation of bilayered ultralight aerogels based on N-rich conjugated microporous polymers nanotubes. *Eur. Polym. J.* **2020**, *126*, 109560.
(73) Wang, Y.; La, A.; Ding, Y.; Liu, Y.; Lei, Y. Novel signal-amplifying fluorescent nanofibers for naked-eye-based ultrasensitive detection of buried explosives and explosive vapors. *Adv. Funct. Mater.* **2012**, *22* (17), 3547−3555.
(74) Xue, J.; Wu, T.; Dai, Y.; Xia, Y. Electrospinning and electrospun nanofibers: Methods, materials, and applications. *Chem. Rev.* **2019**, *119* (8), 5298−5415.
(75) Giang Phan, V.H.; Duong, H. T. T.; Thambi, T.; Nguyen, T. L.; Turabee, Md. H.; Yin, Y.; Kim, S. H.; Kim, J.; Jeong, J. H.; Lee, D. S. Modularly engineered injectable hybrid hydrogels based on protein-polymer network as potent immunologic adjuvant in vivo. *Biomaterials* **2019**, *195*, 100−110.
(76) Jiang, S.; Ma, B. C.; Huang, W.; Kaltbeitzel, A.; Kizisavas, G.; Crespy, D.; Zhang, K. A. I.; Landfester, K. Visible light active nanofibrous membrane for antibacterial wound dressing. *Nanoscale Horiz* **2018**, *3* (4), 439−446.
(77) Razzaque, S.; Cheng, Y.; Hussain, I.; Tan, B. Synthesis of surface functionalized hollow microporous organic capsules for doxorubicin delivery to cancer cells. *Polym. Chem.* **2020**, *11* (12), 2110−2118.
(78) Pagenkopf, B. L.; Krüger, J.; Stojanovic, A.; Carreira, E. M. Mechanistic insights into Cu-catalyzed asymmetric aldol reactions: Chemical and spectroscopic evidence for a metalloenolate intermediate. *Angew. Chem., Int. Ed.* **1998**, *37* (22), 3124−3126.
(79) Ye, S.; Feng, J.; Wu, P. Highly elastic graphene oxide−epoxy composite aerogels via simple freeze-drying and subsequent routine curing. *J. Mater. Chem. A* **2013**, *1* (10), 3495−3502.
(80) Ou, Y.; Xiong, Y.; Hu, Z.; Zhang, Y.; Dong, L. Emerging conjugated radical polymer cathodes with ultra-long cycle life for an entire polymer rechargeable battery. *J. Mater. Chem. A* **2022**, *10* (19), 10373−10382.
(81) Fang, D.; Wang, X.; Zhang, S.; Sheng, L.; Tang, J.; Zhou, J.; Tang, W. Catalyst-free nitro-coupling synthesis of azo-linked conjugated microporous polymers with superior aqueous energy storage capability. *Science China Materials* **2022**, *65* (4), 958−966.
(82) Wu, J.; Wu, Y.; He, Z.; Li, Z.; Huang, H.; Chen, Y.; Liang, G. Conjugated microporous polymers for near-infrared photothermal control of shape change. *Science China Materials* **2021**, *64* (2), 430−439.
(83) Cui, L.; Yu, S.; Gao, W.; Zhang, X.; Deng, S.; Zhang, C.-y. Tetraphenylenthene-based conjugated microporous polymer for aggregation-induced electrochemiluminescence. *ACS Appl. Mater. Interfaces* **2020**, *12* (7), 7966−7973.
(84) Cui, L.; Wang, P.-Y.; Wang, C.-M.; Zhang, C.-Y. Advance in applications of organic polymer. Based electrochemiluminescence in biochemical analysis. *Chinese Journal of Analytical Chemistry* **2021**, *49* (5), 665−675.

https://doi.org/10.1021/acsami.2c10088
ACS Appl. Mater. Interfaces 2022, 14, 39701−39726

(85) Zhang, Q.; Dai, Q.; Li, M.; Wang, X.; Li, A. Incorporation of MnO nanoparticles inside porous carbon nanotubes originated from conjugated microporous polymers for lithium storage. *J. Mater. Chem. A* **2016**, *4* (48), 19132−19139.
(86) Jiang, J.-X.; Trewin, A.; Adams, D. J.; Cooper, A. I. Band gap engineering in fluorescent conjugated microporous polymers. *Chem. Sci.* **2011**, *2* (9), 1777−1781.
(87) Wu, K.; Guo, J.; Wang, C. An elastic monolithic catalyst: A microporous metalloporphyrin-containing framework-wrapped melamine foam for process-intensified acyl transfer. *Angew. Chem., Int. Ed.* **2016**, *55* (20), 6013−6017.
(88) Tan, L.; Tan, B. Functionalized hierarchical porous polymeric monoliths as versatile platforms to support uniform and ultrafine metal nanoparticles for heterogeneous catalysis. *Chem. Eng. J.* **2020**, *390*, 124485.
(89) Lee, J.; Chang, J. Y. Preparation of a compressible and hierarchically porous polyimide sponge via the sol−gel process of an aliphatic tetracarboxylic dianhydride and an aromatic triamine. *Chem. Commun.* **2016**, *52* (68), 10419−10422.
(90) Wang, G.; Uyama, H. Facile synthesis of flexible macroporous polypropylene sponges for separation of oil and water. *Sci. Rep.* **2016**, *6* (1), 21265.
(91) Moon, I. K.; Yoon, S.; Chun, K.-Y.; Oh, J. Highly elastic and conductive N-doped monolithic graphene aerogels for multifunctional applications. *Adv. Funct. Mater.* **2015**, *25* (45), 6976−6984.
(92) Li, Y.; Chen, J.; Huang, L.; Li, C.; Hong, J.-D.; Shi, G. Highly compressible macroporous graphene monoliths via an improved hydrothermal process. *Adv. Mater.* **2014**, *26* (28), 4789−4793.
(93) Gui, X.; Zeng, Z.; Zhu, Y.; Li, H.; Lin, Z.; Gan, Q.; Xiang, R.; Cao, A.; Tang, Z. Three-dimensional carbon nanotube sponge-array architectures with high energy dissipation. *Adv. Mater.* **2014**, *26* (8), 1248−1253.
(94) Kim, K. H.; Oh, Y.; Islam, M. F. Graphene coating makes carbon nanotube aerogels superelastic and resistant to fatigue. *Nat. Nanotechnol.* **2012**, *7* (9), 562−566.
(95) Bonillo, B.; Sprick, R. S.; Cooper, A. I. Tuning photophysical properties in conjugated microporous polymers by comonomer doping strategies. *Chem. Mater.* **2016**, *28* (10), 3469−3480.
(96) Liu, J.; Yee, K.-K.; Lo, K. K.-W.; Zhang, K. Y.; To, W.-P.; Che, C.-M.; Xu, Z. Selective Ag(I) binding, H2S sensing, and white-light emission from an easy-to-make porous conjugated polymer. *J. Am. Chem. Soc.* **2014**, *136* (7), 2818−2824.
(97) Nailwal, Y.; Devi, M.; Pal, S. K. Luminescent Conjugated Microporous Polymers for Selective Sensing and Ultrafast Detection of Picric Acid. *ACS Applied Polymer Materials* **2022**, *4* (4), 2648−2655.
(98) Zhang, P.; Wu, K.; Guo, J.; Wang, C. From hyperbranched polymer to nanoscale CMP (NCMP): Improved microscopic porosity, enhanced light harvesting, and enabled solution processing into white-emitting dye@NCMP films. *ACS Macro Lett.* **2014**, *3* (11), 1139−1144.
(99) Yang, Y.; Urban, M. W. Self-healing polymeric materials. *Chem. Soc. Rev.* **2013**, *42* (17), 7446−7467.
(100) Lan, Y.; Corradini, M. G.; Weiss, R. G.; Raghavan, S. R.; Rogers, M. A. To gel or not to gel: correlating molecular gelation with solvent parameters. *Chem. Soc. Rev.* **2015**, *44* (17), 6035−6058.
(101) Belali, S.; Karimi, A. R.; Hadizadeh, M. Cell-specific and pH-sensitive nanostructure hydrogel based on chitosan as a photosensitizer carrier for selective photodynamic therapy. *Int. J. Biol. Macromol.* **2018**, *110*, 437−448.
(102) Lee, J.; Chang, J. Y. Synthesis of a palladium acetylide-based tubular microporous polymer monolith via a self-template approach: a potential precursor of supported palladium nanoparticles for heterogeneous catalysis. *RSC Adv.* **2018**, *8* (45), 25277−25282.
(103) Wei, H.; Wang, F.; Qian, X.; Li, S.; Hu, Z.; Sun, H.; Zhu, Z.; Liang, W.; Ma, C.; Li, A. Superhydrophobic fluorine-rich conjugated microporous polymers monolithic nanofoam with excellent heat insulation property. *Chem. Eng. J.* **2018**, *351*, 856−866.
(104) Zhu, Z.; Wu, S.; Liu, C.; Mu, P.; Su, Y.; Sun, H.; Liang, W.; Li, A. Ionic liquid and magnesium hydrate incorporated conjugated microporous polymers nanotubes with superior flame retardancy and thermal insulation. *Polymer* **2020**, *194*, 122387.
(105) Wicklein, B.; Kocjan, A.; Salazar-Alvarez, G.; Carosio, F.; Camino, G.; Antonietti, M.; Bergström, L. Thermally insulating and fire-retardant lightweight anisotropic foams based on nanocellulose and graphene oxide. *Nat. Nanotechnol.* **2015**, *10* (3), 277−283.
(106) Chen, L.; Yang, Y.; Jiang, D. CMPs as scaffolds for constructing porous catalytic frameworks: A built-in heterogeneous catalyst with high activity and selectivity based on nanoporous metalloporphyrin polymers. *J. Am. Chem. Soc.* **2010**, *132* (26), 9138−9143.
(107) Xiang, Z.; Xue, Y.; Cao, D.; Huang, L.; Chen, J.-F.; Dai, L. Highly efficient electrocatalysts for oxygen reduction based on 2D covalent organic polymers complexed with non-precious metals. *Angew. Chem., Int. Ed.* **2014**, *53* (9), 2433−2437.
(108) Mandal, K.; Pentelute, B. L.; Bang, D.; Gates, Z. P.; Torbeev, V. Y.; Kent, S. B. H. Design, total chemical synthesis, and X-Ray structure of a protein having a novel linear-loop polypeptide chain topology. *Angew. Chem., Int. Ed.* **2012**, *51* (6), 1481−1486.
(109) Du, X.; Sun, Y.; Tan, B.; Teng, Q.; Yao, X.; Su, C.; Wang, W. Tröger's base-functionalised organic nanoporous polymer for heterogeneous catalysis. *Chem. Commun.* **2010**, *46* (6), 970−972.
(110) Rose, M.; Notzon, A.; Heitbaum, M.; Nickerl, G.; Paasch, S.; Brunner, E.; Glorius, F.; Kaskel, S. N-Heterocyclic carbene containing element organic frameworks as heterogeneous organocatalysts. *Chem. Commun.* **2011**, *47* (16), 4814−4816.
(111) Liao, P.; Cai, G.; Shi, J.; Zhang, J. Post-modified porphyrin imine gels with improved chemical stability and efficient heterogeneous activity in CO2 transformation. *New J. Chem.* **2019**, *43* (25), 10017−10024.
(112) Tan, J.; Wan, J.; Guo, J.; Wang, C. Self-sacrificial template-induced modulation of conjugated microporous polymer microcapsules and shape-dependent enhanced photothermal efficiency for ablation of cancer cells. *Chem. Commun.* **2015**, *51* (98), 17394−17397.
(113) Liu, F.; Liang, W.; Wang, C.; He, J.; Xiao, C.; Zhu, Z.; Sun, H.; Li, A. Superwetting monolithic hypercrosslinked polymers nanotubes with high salt-resistance for efficient solar steam generation. *Sol. Energy Mater. Sol. Cells* **2021**, *221*, 110913.
(114) Yang, R.-X.; Wang, T.-T.; Deng, W.-Q. Extraordinary capability for water treatment achieved by a perfluorous conjugated microporous polymer. *Sci. Rep.* **2015**, *5*, 10155.
(115) Xie, Y.; Huang, W.; Zheng, B.; Li, S.; Liu, Q.; Chen, Z.; Mai, W.; Fu, R.; Wu, D. All-in-one porous polymer adsorbents with excellent environmental chemosensory responsivity, visual detectivity, superfast adsorption, and easy regeneration. *Adv. Mater.* **2019**, *31* (16), 1900104.
(116) Chae, J. A.; Jeong, S.; Kim, H. J.; Tojo, T.; Oh, Y.; Chi, W. S.; Yoon, H.; Kim, H. Fibrous mesoporous polymer monoliths: macromolecular design and enhanced photocatalytic degradation of aromatic dyes. *Polym. Chem.* **2021**, *12* (16), 2464−2470.
(117) Lei, Y.; Tian, Z.; Sun, H.; Zhu, Z.; Liang, W.; Li, A. Self-cleaning and flexible filters based on aminopyridine conjugated microporous polymers nanotubes for bacteria sterilization and efficient PM2.5 capture. *Sci. Total Environ.* **2021**, *766*, 142594.
(118) Wang, S.; Meng, X.; Luo, H.; Yao, L.; Song, X.; Liang, Z. Post-synthetic modification of conjugated microporous polymer with imidazolium for highly efficient anionic dyes removal from water. *Sep. Purif. Technol.* **2022**, *284*, 120245.
(119) Fei, T.; Zhao, H.; Jiang, K.; Zhang, T. Synthesis and humidity sensitive property of cross-linked water-resistant polymer electrolytes. *Sensors and Actuators B-Chemical* **2015**, *208*, 277−282.
(120) Fei, T.; Jiang, K.; Liu, S.; Zhang, T. Humidity sensor based on a cross-linked porous polymer with unexpectedly good properties. *RSC Adv.* **2014**, *4* (41), 21429−21434.
(121) Ma, X.; Wang, Y.; Zhao, T.; Li, Y.; Su, L.-C.; Wang, Z.; Huang, G.; Sumer, B. D.; Gao, J. Ultra-pH-sensitive nanoprobe library

with broad pH tunability and fluorescence emissions. *J. Am. Chem. Soc.* **2014**, *136* (31), 11085−11092.
(122) Liu, Y.; Xu, B.; Sun, S.; Wei, J.; Wu, L.; Yu, Y. Humidity- and photo-induced mechanical actuation of cross-linked liquid crystal polymers. *Adv. Mater.* **2017**, *29* (9), 1604792.
(123) Alsbaiee, A.; Smith, B. J.; Xiao, L.; Ling, Y.; Helbling, D. E.; Dichtel, W. R. Rapid removal of organic micropollutants from water by a porous β-cyclodextrin polymer. *Nature* **2016**, *529* (7585), 190−194.
(124) Yang, T.; Duncan, T. V. Challenges and potential solutions for nanosensors intended for use with foods. *Nat. Nanotechnol.* **2021**, *16* (3), 251−265.
(125) Kortekaas, L.; Ivashenko, O.; van Herpt, J. T.; Browne, W. R. A remarkable multitasking double spiropyran: Bidirectional visible-light switching of polymer-coated surfaces with dual redox and proton gating. *J. Am. Chem. Soc.* **2016**, *138* (4), 1301−1312.
(126) Zhao, Q.; Dunlop, J. W. C.; Qiu, X.; Huang, F.; Zhang, Z.; Heyda, J.; Dzubiella, J.; Antonietti, M.; Yuan, J. An instant multi-responsive porous polymer actuator driven by solvent molecule sorption. *Nat. Commun.* **2014**, *5* (1), 4293.
(127) Mai, W.; Sun, B.; Chen, L.; Xu, F.; Liu, H.; Liang, Y.; Fu, R.; Wu, D.; Matyjaszewski, K. Water-dispersible, responsive, and carbonizable hairy microporous polymeric nanospheres. *J. Am. Chem. Soc.* **2015**, *137* (41), 13256−13259.
(128) Prabhu, P.; Lee, J.-M. Metallenes as functional materials in electrocatalysis. *Chem. Soc. Rev.* **2021**, *50* (12), 6700−6719.
(129) Wang, H.; Chen, J.; Lin, Y.; Wang, X.; Li, J.; Li, Y.; Gao, L.; Zhang, L.; Chao, D.; Xiao, X.; Lee, J.-M. Electronic modulation of non-van der Waals 2D electrocatalysts for efficient energy conversion. *Adv. Mater.* **2021**, *33* (26), 2008422.
(130) Jose, V.; Nsanzimana, J. M. V.; Hu, H.; Choi, J.; Wang, X.; Lee, J.-M. Highly efficient oxygen reduction reaction activity of N-doped carbon−cobalt boride heterointerfaces. *Adv. Energy Mater.* **2021**, *11* (17), 2100157.
(131) Prabhu, P.; Jose, V.; Lee, J.-M. Design strategies for development of TMD-based heterostructures in electrochemical energy systems. *Matter* **2020**, *2* (3), 526−553.
(132) Jose, V.; Hu, H.; Edison, E.; Manalastas, W., Jr; Ren, H.; Kidkhunthod, P.; Sreejith, S.; Jayakumar, A.; Nsanzimana, J. M. V.; Srinivasan, M.; Choi, J.; Lee, J.-M. Modulation of single atomic Co and Fe sites on hollow carbon nanospheres as oxygen electrodes for rechargeable Zn−Air batteries. *Small Methods* **2021**, *5* (2), 2000751.
(133) Fu, G.; Wang, Y.; Tang, Y.; Zhou, K.; Goodenough, J. B.; Lee, J.-M. Superior oxygen electrocatalysis on nickel indium thiospinels for rechargeable Zn−Air batteries. *ACS Materials Letters* **2019**, *1* (1), 123−131.
(134) Chen, J.; Fan, C.; Hu, X.; Wang, C.; Huang, Z.; Fu, G.; Lee, J.-M.; Tang, Y. Hierarchically porous Co/CoxMy (M = P, N) as an efficient Mott−schottky electrocatalyst for oxygen evolution in rechargeable Zn−Air batteries. *Small* **2019**, *15* (28), 1901518.
(135) Fu, G.; Wang, J.; Chen, Y.; Liu, Y.; Tang, Y.; Goodenough, J. B.; Lee, J.-M. Exploring indium-based ternary thiospinel as conceivable high-potential air-cathode for rechargeable Zn−Air batteries. *Adv. Energy Mater.* **2018**, *8* (31), 1802263.
(136) Wang, H.; Li, J.; Li, K.; Lin, Y.; Chen, J.; Gao, L.; Nicolosi, V.; Xiao, X.; Lee, J.-M. Transition metal nitrides for electrochemical energy applications. *Chem. Soc. Rev.* **2021**, *50* (2), 1354−1390.
(137) Zhang, M.; Yu, A.; Wu, X.; Shao, P.; Huang, X.; Ma, D.; Han, X.; Xie, J.; Feng, X.; Wang, B. Sealing functional ionic liquids in conjugated microporous polymer membrane by solvent-assisted micropore tightening. *Nano Research* **2022**, *15* (3), 2552−2557.
(138) Hu, B.; Luo, W.; Zhang, X.-l.; Zhang, B.; Hu, X.-q.; Jin, L. Synthesis and fast switching electrochromic properties of conjugated microporous polymers based on carbazole-thiophene derivatives. *Dyes Pigm.* **2022**, *198*, 109989.
(139) Jayakumar, A.; Jose, V. K.; Lee, J.-M. Hydrogels for medical and environmental applications. *Small Methods* **2020**, *4* (3), 1900735.
(140) Dong, Y.; A, S.; Rodrigues, M.; Li, X.; Kwon, S. H.; Kosaric, N.; Khong, S.; Gao, Y.; Wang, W.; Gurtner, G. C. Injectable and tunable gelatin hydrogels enhance stem cell retention and improve cutaneous wound healing. *Adv. Funct. Mater.* **2017**, *27* (24), 1606619.
(141) Kranz, L. M.; Diken, M.; Haas, H.; Kreiter, S.; Loquai, C.; Reuter, K. C.; Meng, M.; Fritz, D.; Vascotto, F.; Hefesha, H.; Grunwitz, C.; Vormehr, M.; Hüsemann, Y.; Selmi, A.; Kuhn, A. N.; Buck, J.; Derhovanessian, E.; Rae, R.; Attig, S.; Diekmann, J.; Jabulowsky, R. A.; Heesch, S.; Hassel, J.; Langguth, P.; Grabbe, S.; Huber, C.; Türeci, Ö.; Sahin, U. Systemic RNA delivery to dendritic cells exploits antiviral defence for cancer immunotherapy. *Nature* **2016**, *534* (7607), 396−401.
(142) Garcia, D. R.; Lavignac, N. Poly(amidoamine)−BSA conjugates synthesised by Michael addition reaction retained enzymatic activity. *Polym. Chem.* **2016**, *7* (47), 7223−7229.
(143) Wang, H.; Zhu, D.; Paul, A.; Cai, L.; Enejder, A.; Yang, F.; Heilshorn, S. C. Covalently adaptable elastin-like protein−hyaluronic acid (elp−ha) hybrid hydrogels with secondary thermoresponsive crosslinking for injectable stem cell delivery. *Adv. Funct. Mater.* **2017**, *27* (28), 1605609.
(144) Chen, L.; Yang, Y.; Guo, Z.; Jiang, D. Highly efficient activation of molecular oxygen with nanoporous metalloporphyrin frameworks in heterogeneous systems. *Adv. Mater.* **2011**, *23* (28), 3149−3154.
(145) Totten, R. K.; Kim, Y.-S.; Weston, M. H.; Farha, O. K.; Hupp, J. T.; Nguyen, S. T. Enhanced catalytic activity through the tuning of micropore environment and supercritical co2 processing: Al-(porphyrin)-based porous organic polymers for the degradation of a nerve agent simulant. *J. Am. Chem. Soc.* **2013**, *135* (32), 11720−11723.
(146) Kundu, D. S.; Schmidt, J.; Bleschke, C.; Thomas, A.; Blechert, S. A microporous binol-derived phosphoric acid. *Angew. Chem., Int. Ed.* **2012**, *51* (22), 5456−5459.
(147) Yang, Z.-Z.; Zhang, H.; Yu, B.; Zhao, Y.; Ji, G.; Liu, Z. A Tröger's base-derived microporous organic polymer: design and applications in CO2/H2 capture and hydrogenation of CO2 to formic acid. *Chem. Commun.* **2015**, *51* (7), 1271−1274.
(148) Li, Y.; Peng, C.-K.; Hu, H.; Chen, S.-Y.; Choi, J.-H.; Lin, Y.-G.; Lee, J.-M. Interstitial boron-triggered electron-deficient Os aerogels for enhanced pH-universal hydrogen evolution. *Nat. Commun.* **2022**, *13* (1), 1143.
(149) Hu, X.; Chen, Y.; Zhang, M.; Fu, G.; Sun, D.; Lee, J.-M.; Tang, Y. Alveolate porous carbon aerogels supported Co9S8 derived from a novel hybrid hydrogel for bifunctional oxygen electrocatalysis. *Carbon* **2019**, *144*, 557−566.
(150) Fu, G.; Yan, X.; Chen, Y.; Xu, L.; Sun, D.; Lee, J.-M.; Tang, Y. Boosting bifunctional oxygen electrocatalysis with 3D graphene aerogel-supported Ni/MnO particles. *Adv. Mater.* **2018**, *30* (5), 1704609.
(151) Anjali, J.; Jose, V. K.; Lee, J.-M. Carbon-based hydrogels: synthesis and their recent energy applications. *J. Mater. Chem. A* **2019**, *7* (26), 15491−15518.
(152) Zhang, M.; Zhao, T.; Dou, J.; Xu, Z.; Zhang, W.; Chen, X.; Wang, X.; Zhou, B. Bottom-up construction of conjugated microporous polyporphyrin-coated graphene hydrogel composites with hierarchical pores for high-performance capacitors. *Chemelectrochem* **2019**, *6* (24), 5946−5950.